

REF-VLM: Triplet-Based Referring Paradigm for Unified Visual Decoding

Yan Tai¹, Luhao Zhu², Zhiqiang Chen⁴, Yunan Ding³, Yiying Dong³
Xiaohong Liu¹, Guodong Guo⁴

¹Shanghai Jiao Tong University, ²Zhejiang University, ³Hong Kong Polytechnic University

⁴Ningbo Institute of Digital Twin, Eastern Institute of Technology, Ningbo, China

yan.tai@sjtu.edu.cn, aaronzhu@zju.edu.cn

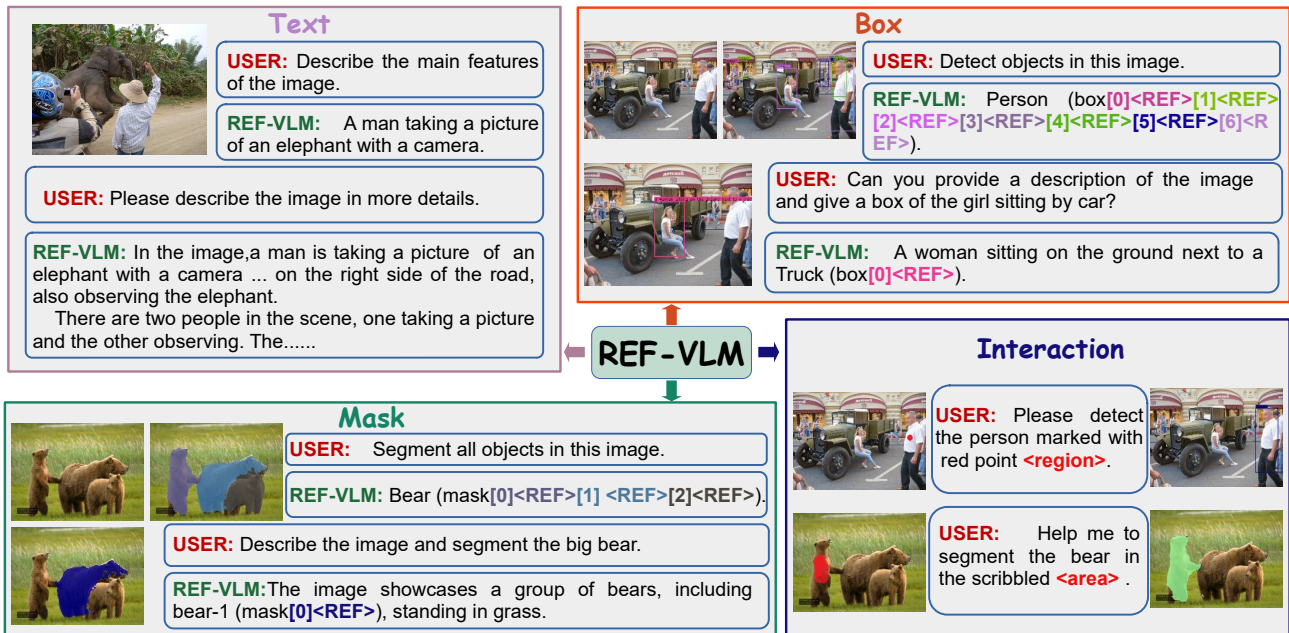


Figure 1. **Overview of Visual Tasks Supported by REF-VLM.** REF-VLM supports a wide range of visual tasks with user-provided visual inputs such as points, boxes, scribbles, and masks, while enabling the decoding of visual contents into formats like points, boxes and masks. For better visualization, details such as TRP and part of special tokens are hidden in the model’s responses.

Abstract

Multimodal Large Language Models (MLLMs) demonstrate robust zero-shot capabilities across diverse vision-language tasks after training on mega-scale datasets. However, dense prediction tasks, such as semantic segmentation and keypoint detection, pose significant challenges for MLLMs when represented solely as text outputs. Simultaneously, current MLLMs utilizing latent embeddings for visual task decoding generally demonstrate limited adaptability to both multi-task learning and multi-granularity scenarios. In this work, we present **REF-VLM**, an end-to-end framework for unified training of various visual decoding tasks. To address complex visual decoding scenarios, we introduce the **Triplet-Based Referring Paradigm (TRP)**, which explic-

itly decouples three critical dimensions in visual decoding tasks through a triplet structure: concepts, decoding types, and targets. TRP employs symbolic delimiters to enforce structured representation learning, enhancing the parsability and interpretability of model outputs. Additionally, we construct **Visual-Task Instruction Following Dataset (VT-Instruct)**, a large-scale multi-task dataset containing over 100 million multimodal dialogue samples across 25 task types. Beyond text inputs and outputs, VT-Instruct incorporates various visual prompts such as point, scribble, and mask, and generates outputs composed of text and visual units like box, keypoint, depth and mask. The combination of different visual prompts and visual units generates a wide variety of task types, expanding the applicability of REF-VLM significantly. Both qualitative and

Table 1. Comparisons of recent MLLMs and their capabilities in performing downstream tasks.

Model	End-to-End	Extensible	Visual Understanding		Referring Expression			Interactive Grounding (IG)		Grounded Conversation Generation (GCG)		Open Vocabulary Identification				
			VQA	Caption	RES	REC	REG	Mask	Box	Mask	Box	OVS	OVD	FOVS	FOVD	
LLaVA [34]	✓	-	✓	✓	-	✓	-	-	-	-	-	-	-	-	-	-
MM-REACT [64]	-	✓	✓	✓	-	✓	✓	-	-	-	✓	-	-	-	-	-
Visual ChatGPT [54]	-	✓	✓	✓	✓	✓	✓	-	-	-	-	✓	✓	✓	✓	✓
HuggingGPT [48]	-	✓	✓	✓	✓	✓	✓	-	-	-	-	-	✓	✓	✓	✓
BuboGPT [74]	-	-	✓	✓	-	✓	-	-	-	-	✓	-	-	-	-	-
Kosmos-2 [41]	✓	-	✓	✓	-	✓	✓	-	-	-	✓	-	-	-	-	-
Shikra [9]	✓	-	✓	✓	-	✓	✓	-	-	-	✓	-	-	-	-	-
MiniGPT-v2 [8]	✓	-	✓	✓	-	✓	✓	-	-	-	✓	-	-	-	-	-
NExT-Chat [70]	✓	-	✓	✓	✓	✓	✓	-	-	✓	✓	-	-	-	-	-
Ferret [66]	✓	-	✓	✓	-	✓	✓	-	✓	-	✓	-	-	-	-	-
SHPINX [31]	-	✓	✓	✓	-	✓	-	-	-	✓	✓	-	-	-	-	-
LLaVA-Plus [35]	✓	✓	✓	✓	✓	✓	-	-	-	-	-	✓	-	-	-	-
LISA [28]	✓	-	✓	✓	✓	✓	-	-	-	-	-	-	-	-	-	-
Osprey [68]	✓	-	✓	✓	-	✓	✓	-	-	-	-	-	-	-	-	-
GLaMM [45]	✓	-	✓	✓	✓	✓	-	-	-	✓	-	-	-	-	-	-
PixelLM [61]	✓	-	✓	✓	✓	✓	-	-	-	✓	-	-	-	-	-	-
PSALM [73]	✓	-	✓	✓	✓	✓	-	✓	✓	-	-	✓	-	-	-	-
GroundHOG [72]	✓	-	✓	✓	✓	✓	✓	-	-	✓	-	-	-	-	-	-
F-LLM [58]	✓	-	✓	✓	✓	✓	-	-	-	✓	-	-	-	-	-	-
VITRON [19]	-	✓	✓	✓	✓	✓	✓	-	-	-	✓	-	-	-	-	-
VisionLLM [52]	✓	-	✓	✓	✓	✓	✓	-	-	✓	✓	-	✓	✓	-	-
VisionLLMv2 [56]	✓	-	✓	✓	✓	✓	✓	✓	✓	✓	✓	-	✓	✓	-	-
REF-VLM (Ours)	✓	✓	✓	✓	✓	✓	✓	✓	✓	✓	✓	✓	✓	✓	✓	✓

quantitative experiments demonstrate that our REF-VLM outperforms other MLLMs across a variety of standard benchmarks. The code, dataset, and demo available at <https://github.com/MacavityT/REF-VLM>.

1. Introduction

Multimodal Large Language Models (MLLMs) demonstrate excellent performance in tasks such as visual question answering and scene understanding [2, 34, 50]. Despite these achievements, typical MLLMs primarily understand input and generate responses with text, which limits their ability to perform fine-grained visual localization. As a result, they struggle to make significant contributions in real-world applications such as autonomous driving, robotics, and medical diagnosis.

In this work, we present **REF-VLM**, an end-to-end framework that enables unified multi-task training, contrasting with existing models that require separate stage-wise training for different tasks, thereby enhancing semantic consistency. To encode diverse user interactions, we introduce a novel *parameter-free Mask-Guided Aggregation* scheme. Additionally, we propose a *Latent Embeddings Router* and *Parallel Group Hungarian Matching* to handle multi-task and multi-granularity decoding scenarios effectively.

As illustrated in Figure 2 (b), conventional Vision Language Models (VLMs) [28, 45, 56] typically generate responses in a simplistic “Visual Concept +

Referring token” format, which proves inadequate for complex multi-granularity scenarios. To address even more challenging visual decoding tasks as shown in Figure 2 (c), we introduce the **Triplet-Based Referring Paradigm (TRP)**, which enforces explicit generation of three core components: (1) visual concept, (2) decoding type, and (3) referring tokens, organized through a structured special token framework. The inherent compositional nature of the triplet structure endows TRP with a “one-fits-all” capability, effectively handling complex multi-task and multi-granularity scenarios. To further enhance the precision of structured text generation, we introduce *Visual Decoding Chain-of-Thought (VD-CoT)*, which requires the model to first overview the image and summarize task-relevant information before generating TRP-compliant responses. The synergistic combination of VD-CoT and TRP significantly improves model performance and accuracy across multi-task visual decoding scenarios.

To enhance the diversity of vision-language tasks, we propose **Visual-Task Instruction Following Dataset (VT-Instruct)**, a multimodal dataset specifically designed to support a wide range of tasks, including Visual Understanding [34], Referring Expressions [9, 66, 70, 73], Interactive Grounding (IG) [56, 73], Open-Vocabulary Identification [48, 54, 56, 73], Grounded Conversation Generation (GCG) [45], Keypoint Detection [31, 56] and Depth Estimation [31]. VT-Instruct consists of more than 100 million high-quality multimodal dialogue samples, primarily derived from pub-

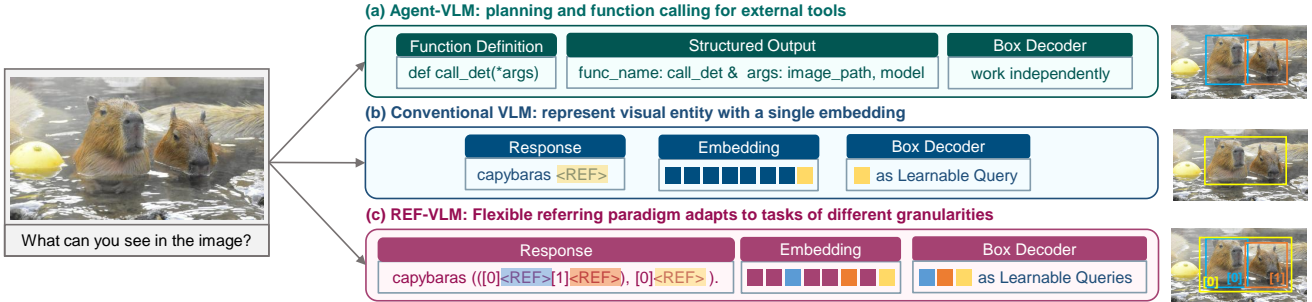


Figure 2. **Comparison of Visual Unit Decoding Methods.** Benefiting from the Triplet-Based Referring Paradigm, REF-VLM can adapt to more complex granularity scenarios and visual decoding tasks, enhancing the interpretability and accuracy of the MLLM’s responses.

licly available datasets such as LAION-5B [47], SA-1B [26], COCO [30], GRIT [41], etc. Each sample is enhanced with thoughtfully crafted prompt templates with multimodal inputs (e.g. images, texts, points, boxes, scribbles and masks) to facilitate instruction following and diverse outputs (e.g. texts, boxes, keypoints, depth and masks) for different downstream tasks.

Our contributions can be summarized as follows:

- We propose **REF-VLM**, an end-to-end framework for unified visual decoding tasks, integrating novel components like Mask-Guided Aggregation, Latent Embeddings Router, and Parallel Group Hungarian Matching to boost multi-task performance and adaptability.
- We design a **Unified Instruction Pipeline** with the Triplet-Based Referring Paradigm and VD-CoT for precise referring in multi-task and multi-granularity scenarios. We also introduce VT-Instruct, a large-scale dataset with 100M multimodal dialogue samples spanning 25 task types, enabling robust understanding and decoding of diverse visual units.
- Extensive experiments show that REF-VLM outperforms existing MLLMs on tasks including Visual Understanding, Referring Expression, Grounded Conversational Generation, Open-Vocabulary Identification, and Interactive Grounding.

2. Related Works

MLLMs often lack the capability to output visual units such as boxes, keypoints, and masks. To expand their applicability in real-world visual tasks, it is typically necessary to implement targeted designs for different visual tasks.

Decode Visual Units with Agent Tools. Another approach involves using the MLLM as an agent to coordinate task-specific models, enabling localization of visual targets [35]. In this case, MLLM outputs textual descriptions of recognized content and scheduling results, which can be utilized by downstream visual tools. LLaVa-Plus [35] constructs an instruction-following dataset that includes a large number of

samples for using task-specific models as tools. VITRON [19] incorporates a sketch encoder to process user-provided visual prompts and supports direct generation of bounding box coordinates by the model. However, since the final visual unit is derived from the tool models, there may be a gap between the MLLM’s understanding and the final output. Moreover, the model is unable to effectively leverage previous visual recognition results during prediction, requiring repeated input of tool model outputs, leading to issues such as insufficient robustness and accuracy in multi-task and multi-target applications.

Decode Visual Units with Latent Embeddings. Using the tokens output by the MLLM as learnable queries input into task-specific decoders is the most widely adopted visual decoding strategy [28, 45]. LISA [28] adopts SAM [26] as the mask decoder, where MLLM generates learnable special tokens as prompts for SAM, producing fine-grained segmentation results. PSALM [73] divides the input for open-vocabulary segmentation tasks into instruction prompts, condition prompts, and discrete mask tokens, decoding the output mask tokens to obtain segmentation results aligned with the prompt content. GLAMM [45] integrates text-based dialogue with segmentation tasks, utilizing SAM to simultaneously generate detailed descriptions and mask results from the model. VisionLLM v2 [56] introduces the super-link technique, where the MLLM generates task-specific special tokens to serve as routing tokens. These tokens are followed by additional learnable queries appended to them, facilitating visual decoding tasks.

3. Unified Instruction Pipeline

3.1. Triplet-Based Referring Paradigm

Section 2 describes two dense prediction decoding approaches: “Agent Tools” and “Latent Embeddings”. As shown in Figure 2(a), MLLMs act as agents, generating structured text (e.g., JSON) to invoke external decoders like Grounding DINO [36] and SAM [26]. Meanwhile, Figure 2(b) and (c) depict the Latent Embeddings approach,


<p>Prompt Share your perspective of the scene and give the bounding box for each object you discuss. Please give me a detailed rundown.</p>	
<p>VD-CoT <Task> Unit decode (True). Class name, target unit and number: - Name: electric boat Unit: box Num: 1 - Name: two men Unit: box Num: 2 - Name: baseball cap Unit: box Num: 2 - Name: red apple Unit: box Num: 1 </Task></p>	
<p>Answer with Triplets <Phrase>Two men</Phrase> (<Unit>box</Unit>[0] <REF>[1]<REF>) wearing <Phrase>baseball caps</Phrase> (<Unit>box</Unit>[0] <REF>[1]<REF>) stand on an <Phrase>electric boat</Phrase>(<Unit>box</Unit>[0]<REF>), with one holding a <Phrase>red apple</Phrase>(<Unit>box</Unit>[0]<REF>).</p>	

Table 2. An Example of VD-CoT Applied to the Grounded Conversation Generation (GCG) Task. VD-CoT analyzes the image and outputs the structured visual decoding information required by TRP. The answer is generated synchronously with the triplet, and the special tokens have been simplified in the example.

where MLLM outputs serve as learnable queries for visual task decoders. Here, the special token <REF> facilitates referential learning. Our REF-VLM adopts the Latent Embeddings framework, offering greater flexibility and adaptability for diverse visual decoding tasks. For clarity, we omit some special tokens used for assisting referential tasks.

In Figure 2(b), we illustrate the conventional referring paradigm [28, 45, 46, 56], where the <REF> token is typically introduced after visual concepts to enable a single decoding process. However, discrete labels suffer from semantic ambiguity. For instance, the phrase “People are crossing the street” can refer to visual concepts such as the entire scene (single target), the people (multiple targets) and the street (single target). Existing reference schemes struggle to effectively handle visual concept references at different granularities, ultimately impacting the interpretability and accuracy of MLLM responses. Moreover, since different visual tasks require varying decoding granularities, extending the “Latent Embeddings” decoding approach to multi-task scenarios necessitates a more effective referring and embedding framework.

We propose the **Triplet-Based Referring Paradigm (TRP)**, a mechanism for multi-granularity visual concept decoding. As shown in Figure 2(c), TRP resolves semantic ambiguity and supports multi-granularity referencing in visual tasks. TRP comprises three components: (i) *Visual Concepts*, encapsulated in <Phrase> tags (e.g., <Phrase>dogs</Phrase>); (ii) *Decoding Types*, specified in <Unit> tags (e.g., <Unit>box</Unit>); and (iii) *References*, denoted by <REF> to link concepts to instances (e.g., [0]<REF> for the first detected dog). Consequently, the example in Figure 2(c) corresponds to the full representation: <Phrase>capybaras</Phrase>((<Unit>box</Unit>[0]<REF>[1]<REF>), <Unit>box</Unit>[1]<REF>).

The TRP framework demonstrates a “one-fits-all” advantage across diverse visual tasks. This is achieved through two key design strengths: (1) **Syntactic Scalability**: The triplet-based structure inherently supports compositional expansion. TRP can represent complex scene descriptions through hierarchical nesting, such as “<Phrase><Phrase>dog</Phrase> in <Phrase>park</Phrase></Phrase>”. Additionally, TRP can specify composite tasks by combining multiple “<Unit>” tags (e.g., “<Unit>box, keypoint</Unit>”). (2) **Task Extensibility**: By pre-defining the semantic space of “<Unit>” tags (e.g., introducing “<Unit>depth</Unit>”), TRP enables zero-shot task extension, allowing seamless adaptation to new visual tasks without additional training [50]. These design strengths ensure that TRP is not only versatile but also future-proof, making it a robust solution for multi-granularity visual concept decoding.

3.2. Visual Decoding Chain-of-Thought

TRP enforces structured representation learning through symbolic delimiters, enhancing the parsability and interpretability of the output. To further improve the accuracy of the triplet-structured output, we introduce the **Visual Decoding Chain-of-Thought (VD-CoT)**, an instruction-tuning approach designed to guide TRP generation.

As shown in Table 2, the VD-CoT process is encapsulated within “<Task>” and “</Task>” tags. When executing visual decoding tasks, VD-CoT requires the MLLM to: (1) Identify the visual concepts to be decoded. (2) Specify the type of decoding required for the current task. (3) Determine the number of instances to be decoded. When no decoding task is needed, VD-CoT simply outputs “Unit decode (False).” This structured approach ensures precise and context-aware generation, further enhancing TRP’s effectiveness in multi-granularity visual concept decoding.

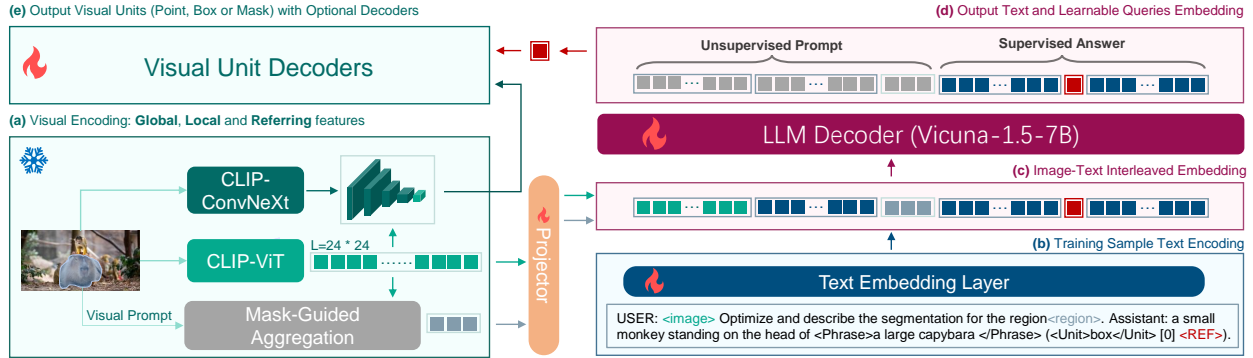


Figure 3. **The Framework of REF-VLM.** REF-VLM employs dual-architecture visual encoders to jointly encode images into a feature pyramid, enhancing visual unit decoder performance. Additionally, visual prompts are fused with global features and share a projector, enabling parameter-free encoding of image interactions. Training samples adhere to the Triplet-Based Referring Paradigm, ensuring one-to-one mapping between REF-VLM’s latent embeddings and decoding targets.

Definitions and roles of all special tokens used in RE-VLM are detailed in Appendix Table 10.

3.3. Visual-Task Instruction Following Dataset

Following the Triplet-Based Referring Paradigm, We present **Visual-Task Instruction Following Dataset (VT-Instruct)**, a large-scale visual multi-task dataset that combines different visual prompts as inputs and visual units as outputs. VT-Instruct comprises over 100 million dialogue samples featuring multimodal input-output pairs. These pairs encompass various combinations of output units, ranging from low to high visual density, including point, box, keypoint, depth and mask, combined with either low or high text complexity.

For each downstream task, we (i) first construct a specific system instruction and (ii) generate over 150 task-specific prompt templates using GPT-4, randomly selecting them to construct user prompts, then (iii) we modify existing dataset annotations to construct a unified answering format following the rule of TRP (Section 3.1), creating multi-turn conversations featuring a system-prompt-answer combination.

Due to efficiency and computational resource considerations, REF-VLM utilizes only a small subset of VT-Instruct as its training set. As a visual decoding task framework, **REF-VLM’s training samples are generally comparable to or fewer than those in similar studies [2, 5, 11, 45, 46, 56, 68, 73] for each individual task.** For an analysis of VT-Instruct dataset usage, please refer to the Appendix Table 16. The details of definition for each task will be presented in Appendix B.

4. End-to-End Decoding Framework

Unlike existing “Latent Embeddings” decoding methods that require task-specific fine-tuning in separate stages [56], REF-VLM achieves *unified end-to-end training* for all tasks, including conventional QA, VQA, and various visual decod-

ing tasks. We will illustrate the training process using an example based on the Referring GCG-Segmentation task and discuss the core components of the framework in the following subsections.

4.1. Unified Training Workflow

The example training task in Figure 3 requires the MLLM to describe a user-specified region based on a mask and prompt input, and generate precise segmentation results.

REF-VLM supports image and visual prompt (VPT) inputs, where VPT includes point, box, scribble, and mask. For image encoding, we follow LLaVA [34] and use CLIP-ViT [44] to extract global features mapped to the text embedding space. To address CLIP-ViT’s limitations [28, 45, 73] in dense prediction tasks, we additionally employ CLIP-ConvNeXt [14], a Conv-based architecture pre-trained on large-scale image-text pairs, to capture multi-scale local features. The outputs of both encoders are concatenated to improve visual task decoding. For VPT encoding, we propose a parameter-free *Mask-Guided Aggregation* method (see Section 4.2) to fuse image and VPT features, enabling precise region understanding.

REF-VLM employs Vicuna-v1.5-7B [75] as the base LLM for processing the text modality. Figure 3(b), (c), and (d) illustrate the parallel decoding and supervision process of a training sample. In the (b) *Training Sample Text Encoding* process, the input training text adheres to the TRP specification outlined in Section 3.1, requiring the LLM to generate a sequence of latent embeddings of equal length for the final visual decoding target, represented as <REF> tokens. In pipeline (c) *Image-Text Interleaved Embedding*, the image global features and aggregated visual prompt features output from pipeline (a) *Visual Encoding* are substituted into the reserved placeholders (i.e., <image> and <region>) respectively, forming a complete sequence fed into the LLM Decoder.

Figure 3(d) and (e) illustrates the supervision process of the training sequence. The gray area corresponds to the prompt part, which does not require loss calculation during the supervised fine-tuning. The blue area corresponds to the answer part, which is mapped to the vocabulary and included in the loss computation. The red area corresponds to the $\langle \text{REF} \rangle$ tokens, which not only undergo the same LLM loss calculation as the blue area but also serve as inputs to the visual unit decoders for further decoding. This aspect will be detailed in Section 4.3.

REF-VLM follows a two-stage training process. In the first stage, similar to Shikra [9], only the global visual encoder (CLIP-ViT), the projector, and the LLM participate in computation. During this phase, the weights of CLIP-ViT and the LLM remain fixed, with only the projector’s parameters being updated. In the second stage, REF-VLM is trained in a unified manner across all tasks. Beyond the modules in the (a) *Visual Encoding pipeline*, all other components, including the projector, LLM, and visual unit decoders are updated. The Unified Training Workflow of REF-VLM offers better semantic consistency compared to similar approaches that rely on pre-trained visual task decoders [28, 45, 46, 56, 68], such as SAM [26] or Grounding-DINO [36]. REF-VLM eliminates the need to repeatedly use visual encoders for each visual task, significantly reducing the overall model parameters. This aspect will be discussed in detail in Appendix C.

4.2. Mask-Guided Aggregation

REF-VLM achieves diverse referencing tasks through visual prompt support (points, boxes, scribbles, masks). Unlike existing methods requiring additional parameters [19, 68], we introduce **parameter-free Mask-Guided Aggregation**. First, we perform two steps: (1) converting prompts into normalized masks whose sizes are aligned with global features; (2) partitioning features and masks into grids for patch-wise fusion.

Let the input image global features be denoted as $\mathcal{X} \in \mathbb{R}^{C \times N \times H \times W}$, where C is the number of channels, N indicates the count of spatial patches, and $H \times W$ define the spatial resolution of each patch. Given a mask $\mathcal{M} \in \mathbb{R}^{Q \times N \times H \times W}$ with Q representing the embedding length used to encode the features of visual prompts, our aggregation operation computes an Hadamard product between channel-aligned features (\mathcal{X}) and query-specific masks (\mathcal{M}) at each spatial position (h, w) , followed by summation over the $H \times W$ dimensions.

$$\mathcal{V}_{q,n,c} = \sum_{h=1}^H \sum_{w=1}^W \mathcal{X}_{c,n,h,w} \cdot \mathcal{M}_{q,n,h,w} \quad (1)$$

Let the aggregated output tensor be $\mathcal{V} \in \mathbb{R}^{Q \times N \times C}$. To inject spatial awareness, we augment it with cosine positional

encodings. For position index n and channel c , the encoding is defined as:

$$\text{PE}(n, c) = \cos\left(\frac{n}{s^{2c/C}}\right), \quad (2)$$

where s is a temperature hyperparameter. The refined features $\tilde{\mathcal{V}}$ are obtained by:

$$\tilde{\mathcal{V}}_{q,n,c} = \mathcal{V}_{q,n,c} + \alpha \cdot \text{PE}(n, c), \quad (3)$$

where α could be a learnable scalar, but in our setup, α is set to a constant value of 1.

Finally, the visual prompt features and image global features share the projector layer, achieving efficient feature fusion without introducing additional parameters.

4.3. Visual Unit Decoders

In unified multi-task training, each batch instance undergoes task-specific decoding processes. Figure 4 illustrates REF-VLM’s workflow, showing a single sample requiring dual-task decoding. For clarity, we omit components detailed in Section 4.1.

Figure 4(a) shows REF-VLM’s training pipeline: (1) visual data passes through dual encoders to build a feature pyramid, aligning with Section 4.1; (2) the LLM processes prompts, generating TRP-structured responses (Section 3.1) with $\langle \text{REF} \rangle$ tokens for one-to-one referring between latent embeddings and visual instances. The LLM embeddings are categorized as: gray (text tokens), red (box targets embeddings), and blue (mask targets embeddings). We leverage the *Latent Embeddings Router* to filter task-specific embeddings, which are then padded to a fixed length before being fed into their respective visual decoders. The TRP’s one-to-one mapping enables exclusion of padding tokens from loss computation.

For both box and mask decoders, we adopt streamlined yet effective architectures: DETR [6] for box prediction and MaskFormer [12] for mask segmentation. As illustrated in Figure 4(a) and (b), the image feature pyramid undergoes fusion and flattening operations before serving as input to the transformer decoder, which jointly processes the features with latent embeddings for visual unit decoding. However, given the distinctive properties of the TRP mechanism - particularly its inherent one-to-one correspondence between embeddings and targets - this introduces two significant modifications to the decoding process: (1) Each prediction is uniquely associated with a decoding target, thereby eliminating the need for a classification head; (2) The TRP inherently partitions predictions into distinct groups, rendering the standard Hungarian matching algorithm [6] inadequate. A critical challenge arises when multiple targets exist within a single group, as exemplified by the ‘capybaras’ group containing two bounding boxes: how to determine the optimal matching configuration? To address issue (1), we eliminate

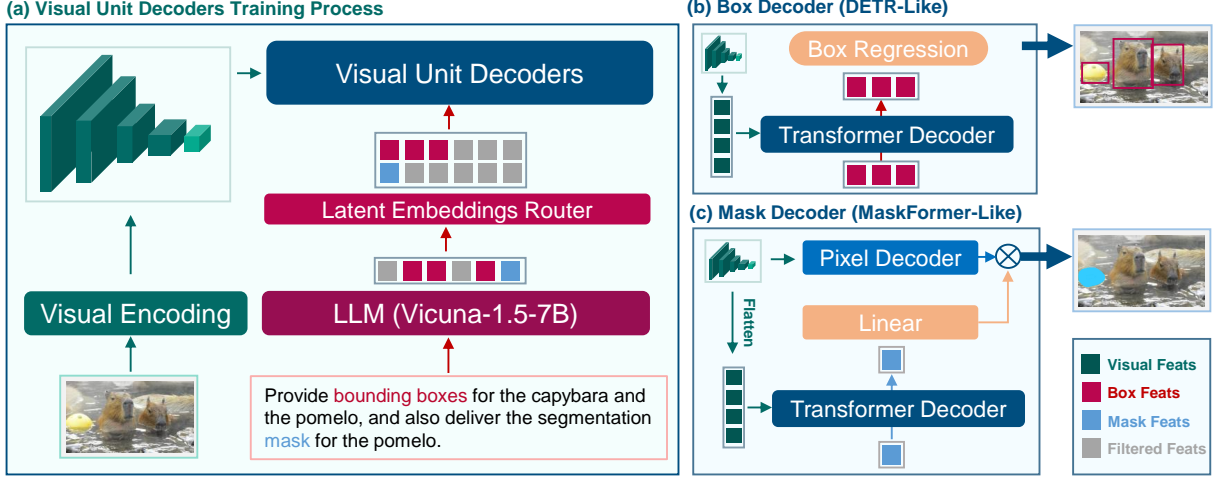


Figure 4. **Architecture of Visual Unit Decoders.** We propose a Latent Embeddings Router to facilitate unified multi-task training in REF-VLM, and enhance the Hungarian matching algorithm for the TRP-based one-to-one referring decoding scheme.

the classification layers from both the box and mask decoders. For issue (2), we propose a novel *Parallel Grouped Hungarian Matching* strategy to ensure precise alignment between predictions and ground truth annotations.

Let \mathcal{B} denote a batch containing B independent groups. For the i -th group: (i) $\mathbf{P}^{(i)} = \{\mathbf{p}_1^{(i)}, \dots, \mathbf{p}_{N_i}^{(i)}\}$: Set of N_i predicted boxes. (ii) $\mathbf{T}^{(i)} = \{\mathbf{t}_1^{(i)}, \dots, \mathbf{t}_{M_i}^{(i)}\}$: Set of M_i target boxes. (iii) $\mathcal{C}^{(i)} \in \mathbb{R}^{N_i \times M_i}$: Cost matrix where element $c_{nm}^{(i)}$ represents the matching cost between $\mathbf{p}_n^{(i)}$ and $\mathbf{t}_m^{(i)}$. (iv) $\sigma^{(i)} : \{1, \dots, N_i\} \rightarrow \{1, \dots, M_i\} \cup \{\emptyset\}$: Injective matching function for the i -th group.

The pairwise cost combines geometric measures:

$$c_{nm}^{(i)} = \lambda_{\text{LI}} \mathcal{L}_{\text{LI}}(\mathbf{p}_n^{(i)}, \mathbf{t}_m^{(i)}) + \lambda_{\text{IoU}} \mathcal{L}_{\text{IoU}}(\mathbf{p}_n^{(i)}, \mathbf{t}_m^{(i)}) \quad (4)$$

where λ_{LI} and λ_{IoU} are weighting coefficients, \mathcal{L}_{LI} denotes normalized coordinate differences, and \mathcal{L}_{IoU} represents the generalized IoU loss.

To enable parallel computation, we construct a padded tensor:

$$\tilde{\mathcal{C}} \in \mathbb{R}^{B \times N_{\max} \times M_{\max}} \quad (5)$$

where $N_{\max} = \max(N_i)$ and $M_{\max} = \max(M_i)$. Invalid entries are masked using:

$$\mathbf{M}_{nm}^{(i)} = \begin{cases} 0 & n \leq N_i \wedge m \leq M_i \\ -\infty & \text{otherwise} \end{cases} \quad (6)$$

For each group i , find optimal permutation matrix $\tilde{\mathbf{A}}^{(i)} \in \{0, 1\}^{N_{\max} \times M_{\max}}$ that minimizes:

$$\sum_{n=1}^{N_{\max}} \sum_{m=1}^{M_{\max}} \tilde{\mathcal{C}}_{nm}^{(i)} \tilde{\mathbf{A}}_{nm}^{(i)} \quad (7)$$

subject to:

$$\sum_{m=1}^{M_{\max}} \tilde{\mathbf{A}}_{nm}^{(i)} \leq 1 \quad \forall n, \quad \sum_{n=1}^{N_{\max}} \tilde{\mathbf{A}}_{nm}^{(i)} \leq 1 \quad \forall m \quad (8)$$

5. Experiments

We conduct quantitative evaluations of our REF-VLM in Section 5.1 and Appendix F.1: (i) Visual Understanding, (ii) Grounded Conversation Generation (GCG), (iii) Referring Expression, (iv) Freeform Open-Vocabulary Identification, (v) Interactive Grounding. Then, we perform ablation studies to evaluate the effectiveness of the key elements in our approach in Section 5.2 and Appendix F.2.

5.1. Quantitative Results

Visual Understanding. We begin by presenting quantitative comparisons on zero-shot image captioning tasks using the Flickr30k [42] and NoCaps [1] validation datasets, as well as VQA tasks on the VQAv2 [3] and OK-VQA [39] test datasets. For image captioning, we report the CIDEr score, while for VQA tasks, overall accuracy is provided. The summarized results in Table 3 demonstrate that our REF-VLM model achieves the highest performance on the image captioning task, with a CIDEr score of 96.0 on the Flickr30k dataset and 122.4 on the NoCaps dataset. For VQA tasks, REF-VLM outperforms other models, achieving 62.39% accuracy on the OK-VQA test dataset and 81.6% on the VQAv2 test dataset, comparable to VisionLLMv2-Chat [56]. Furthermore, we utilize the POPE benchmark [29] to assess hallucination performance in REF-VLM, as shown in Table 5, where REF-VLM attains the highest F1 score, surpassing other MLLMs in every case.

Grounded Conversation Generation (GCG). The

Table 3. Evaluation on Image Captioning and VQA for MLLMs.

Model	Image Captioning		VQA	
	Flickr30K	NoCaps	VQAv2	OKVQA
Flamingo-80B [2]	67.2	-	56.3	50.6
InstructBLIP [16]	82.8	121.9	-	-
LLaVA-1.5-7B [34]	-	-	78.5	54.40
Shikra-13B [9]	73.9	-	77.4	47.16
InternVL-G [11]	79.2	113.7	80.2	-
Qwen-VL [5]	85.8	121.4	78.2	-
VisionLLMv2-Chat [56]	88.7	118.1	81.4	-
VisionLLMv2 [56]	90.2	116.9	80.8	-
GLaMM [45]	95.3	106.8	-	-
REF-VLM	96.0	122.4	81.6	62.39

Table 4. REG Comparison on RefCOCOg.

Model	CIDEr	Meteor
GRiT [57]	71.6	15.2
Kosmos-2 [41]	62.3	14.1
ASM [53]	103.0	20.8
RegionGPT [23]	109.9	16.9
PixelLLM [61]	82.3	14.3
GLaMM [45]	106.0	16.2
Osprey [68]	108.3	16.6
Groma [38]	107.3	16.8
VisionLLMv2-Chat [56]	118.5	21.2
VisionLLMv2 [56]	111.6	20.4
REF-VLM	119.1	21.6

Table 5. Object hallucination benchmark in three POPE [29] evaluation settings.

Sampling	Metrics	REF-VLM	GroundHOG [72]	LION [7]	Osprey [68]	Ferret [66]	Shikra [9]	LLaVA-1.5 [34]	Instruct-BLIP [16]	MiniGPT4 [8]	mPLUG-Owl [65]
Random	Accuracy	92.44	91.03	88.97	89.47	90.24	86.90	88.73	88.57	79.67	53.97
	Precision	90.00	85.80	97.12	93.40	97.72	94.40	88.89	84.09	78.24	52.07
	Recall	96.00	96.40	81.00	84.93	83.00	79.26	88.53	95.13	82.20	99.60
	F1 Score	92.90	90.79	88.33	88.97	89.76	86.19	88.71	89.27	80.17	68.39
Popular	Accuracy	90.10	90.13	86.77	87.83	84.90	83.97	85.83	82.77	69.73	50.90
	Precision	85.78	85.93	91.69	89.94	88.24	87.55	83.91	76.27	65.86	50.46
	Recall	96.13	93.81	80.87	85.20	80.53	79.20	88.67	95.13	81.93	99.40
	F1 Score	90.66	89.70	85.94	87.50	84.21	83.16	86.22	84.66	73.02	66.94
Adversarial	Accuracy	87.30	86.33	85.37	85.33	82.36	83.10	72.10	65.17	79.20	50.67
	Precision	91.54	85.93	88.69	85.43	83.60	85.60	74.69	65.13	61.19	50.34
	Recall	82.20	86.63	81.07	85.20	80.53	59.60	88.34	95.13	82.93	90.33
	F1 Score	86.62	86.28	84.71	85.31	82.00	82.49	80.94	77.32	70.42	66.82

Table 6. REF-VLM performance on Grounding Conversation Generation (GCG) task. Evaluation Metrics for GCG Tasks: CIDEr, Meteor, AP50, mIoU, and Recall. ‘‘Scratch’’ indicates whether the decoder is trained from scratch or utilizes a pretrained visual decoder (e.g., SAM [26], Mask2Former [12]). A ✓ symbol indicates that the visual decoder in REF-VLM was trained from scratch, showcasing that REF-VLM outperforms models using pretrained decoders for generating boxes or masks.

Model	Dataset	Type	Scratch	Val					Test				
				CIDEr	Meteor	AP50	mIoU	Recall	CIDEr	Meteor	AP50	mIoU	Recall
BuboGPT [74]	Grand _f	Mask	✗	3.6	17.2	19.1	54.0	29.4	3.5	17.1	17.3	54.1	27.0
Kosmos-2 [41]		Mask	✗	27.6	16.1	17.1	55.6	28.3	27.2	15.8	17.2	56.8	29.0
LISA [28]		Mask	✗	33.9	13.0	25.2	62.0	36.3	32.2	12.9	24.8	61.7	35.5
GLaMM [45]		Mask	✗	47.2	16.2	30.8	66.3	41.8	37.9	14.6	27.2	64.6	38.0
REF-VLM		Mask	✓	56.9	18.4	26.2	57.9	50.0	53.2	21.7	27.7	56.6	45.3
REF-VLM	Flickr30k	Box	✓	-	-	-	-	-	82.0	26.0	35.4	66.1	47.7

Grounded Conversation Generation (GCG) task consists of two components: GCG-mask and GCG-box. For the GCG-mask task, we further finetune our REF-VLM on the Grand_f [45] training dataset and evaluate its performance on the Grand_f validation and test splits, following the process outlined by [45]. The results presented in Table 6 demonstrate that our REF-VLM, trained from the scratch outperforms current baseline methods which applied pretrained visual decoders, such as GLaMM [45], across metrics including CIDEr, Meteor, AP50, and Recall. Additionally, we assess the GCG-box task using the Flickr30k [42] test set, due to the lack of available MLLMs for the GCG-box task, we only report our zero-shot performance on this dataset.

Referring Expression. We evaluate Referring Expression Generation (REG) on the RefCOCOg test dataset [25], using Meteor and CIDEr as evaluation metrics. The results, shown in Table 4, indicate that our REF-VLM outperforms the State-of-Art (SOTA) MLLM VisionLLMv2-Chat [56]. Additionally, we assess both Referring Expression Comprehension (REC) and Referring Expression Segmentation (RES) tasks in Appendix F.1, demonstrating that REF-VLM achieves the highest performance across these tasks.

Freeform Open-Vocabulary Identification. Compared to existing MLLMs, which generally require category prompts to be added in open-vocabulary tasks [56, 73], enabling the model to understand potential categories in the image before performing open-set detection or segmentation, our

Table 7. **Evaluation on zero-shot open-vocabulary tasks.** Evaluation of Open-Vocabulary Instance Segmentation on the ADE20k Dataset and Object Detection on COCO2017. Since no existing MLLM can perform zero-shot open-vocabulary object detection using a straightforward template without prompting any class hint, we report only our model’s performance on this dataset.

Model	Type	Scratch	Mask Decoder	Box Decoder	ADE20k	COCO
MaskCLIP [18]	SEG	✓	MaskCLIP	-	6.0	-
ODISE [60]	SEG	✓	Diffusion UNet	-	14.4	-
SAN [62]	SEG	✓	CLIP+SAN	-	10.6	-
PSALM [73]	SEG	✗	Mask2Former	-	9.0	-
PSALM+LVIS [73]	SEG	✗	Mask2Former	-	13.9	-
REF-VLM (mAP _S)	SEG/DET	✓	MaskFormer	DETR	16.7	26.7

Table 8. **Comparison across visual encoder and ablation study on group matchers.** [0,1,2,3] means we choose all four feature layers from CLIP-ConvNeXt model, -2 means we only choose CLIP-ViT second last layer, [0,1,2,4] means we concatenate the first three feature layers from CLIP-ConvNeXt and the output feature map from CLIP-ViT. ✓ means we applied the Group Hungarian Matcher when we trained the decoder.

Visual Encoder	Size	Group Matcher	Feature Dimension	cIoU
ConvNeXt-L	320	✓	[0,1,2,3]	41.94
ConvNeXt-L	336	✓	[0,1,2,3]	46.08
CLIP-ViT	336	✓	-2	60.44
ConvNeXt-L + CLIP-ViT	320	✓	[0,1,2,4]	60.02
ConvNeXt-L + CLIP-ViT	512	✗	[0,1,2,4]	61.83
ConvNeXt-L + CLIP-ViT	512	✓	[0,1,2,4]	62.49

Table 9. **CoT ablation study on SA-1B subsets.** The accuracy of the LLM’s output categories and special tokens was assessed under both conditions (with and without CoT) using CIDEr and Meteor as evaluation metrics.

	FOVS		FOVD		GCG_Box		GCG_Mask	
	CIDEr	Meteor	CIDEr	Meteor	CIDEr	Meteor	CIDEr	Meteor
No CoT	25.60	34.45	21.30	31.66	197.88	47.88	204.78	47.77
CoT	27.57	34.22	24.90	27.14	200.72	47.98	205.80	48.23

REF adopts a more flexible approach. With REF-VLM, there is no need to predefine categories, we simply input the prompt like “Please detect bounding boxes (segment objects) in the image<image>”. With this prompt, REF-VLM can autonomously identify potential categories within the image through its LLM, handing off decoding tasks to the subordinate visual decoder. We refer to this more adaptable task as *Freeform Open-Vocabulary Identification* (detail in Appendix E.1). Unlike other MLLMs [56, 73], REF-VLM allows the LLM to directly output categories instead of having the downstream decoder output category names and confidence scores. Accordingly, we introduce mAP_S as a metric (detailed in Appendix E.2) for evaluating REF-VLM’s performance on this task and use it for comparison with other MLLMs. We evaluate REF-VLM on the ADE20k test dataset for

zero-shot freeform open-vocabulary segmentation task and COCO2017 validation dataset for object detection. The results for both tasks are presented in Table 7. Notably, REF-VLM achieves strong performance without any specialized design, outperforming other MLLMs (e.g., PSALM [73]) and specialist models (e.g., SAN [62]). Additionally, REF-VLM also demonstrates the capability to perform open-vocabulary object detection.

5.2. Ablation Study

To assess our framework’s effectiveness, we analyze the impact of group matcher configuration, visual encoder selection, and CoT implementation. We also evaluate various mask token configurations on Mask-Guided Aggregation and test the Group Matcher on more challenging freeform object detection tasks in Appendix F.2.

Choose of Group Matchers. To validate the effectiveness of our Group Hungarian Matcher, we perform an ablation study on its usage in the mask decoder for the RES task, using the RefCOCOg test dataset and cIoU as the evaluation metric. As shown in Table 8, applying the Group Hungarian Matcher for loss computation yields a significantly better performance compared to configurations without it, demonstrating its substantial impact on improving the overall accuracy.

Different Configuration of Visual Encoders. To investigate the effect of different configurations of CLIP vision encoders, including CLIP-ConvNeXt and CLIP-ViT, along with variations in image size and feature selection layers, we conduct experiments on the RES task using the RefCOCOg test dataset. As shown in Table 8, REF-VLM achieves the highest performance when concatenating the CLIP-ConvNeXt and CLIP-ViT encoders with the setting of image size as 512×512.

Choose of CoT. Our ablation study of CoT vs. non-CoT models (1,000 SA-1B images [26]) in Table 9 showed CoT significantly improved performance across all dense prediction tasks, demonstrating enhanced contextual understanding and object recognition.

6. Limitations and Conclusion

In conclusion, this paper introduces REF-VLM, a powerful and extensible open-ended visual multi-task learning framework; TRP, a compositional and extensible “one-fits-all” referring paradigm for visual decoding tasks; VT-Instruct, a large-scale multimodal instruction-tuning dataset. Extensive experiments validate the effectiveness of our REF-VLM. However, despite TRP’s theoretical support for multiple tasks, the actual implemented tasks remain limited. Additionally, performance degradation in multi-turn dialogues and the ratio of data used in training are areas that require further analysis and refinement. Given the aforementioned limitations, our future work will focus on expanding task coverage, enhancing multi-turn dialogue robustness, and optimizing data utilization.

References

- [1] Harsh Agrawal, Karan Desai, Yufei Wang, Xinlei Chen, Rishabh Jain, Mark Johnson, Dhruv Batra, Devi Parikh, Stefan Lee, and Peter Anderson. Nocaps: Novel object captioning at scale. In *Proceedings of the IEEE/CVF international conference on computer vision*, pages 8948–8957, 2019. 7
- [2] Jean-Baptiste Alayrac, Jeff Donahue, Pauline Luc, Antoine Miech, Iain Barr, Yana Hasson, Karel Lenc, Arthur Mensch, Katherine Millican, Malcolm Reynolds, et al. Flamingo: a visual language model for few-shot learning. *Advances in neural information processing systems*, 35:23716–23736, 2022. 2, 5, 8
- [3] Stanislaw Antol, Aishwarya Agrawal, Jiasen Lu, Margaret Mitchell, Dhruv Batra, C. Lawrence Zitnick, and Devi Parikh. Vqa: Visual question answering. In *International Conference on Computer Vision (ICCV)*, 2015. 7, 3, 4
- [4] Bruno Artacho and Andreas Savakis. Unipose: Unified human pose estimation in single images and videos. In *Proceedings of the IEEE/CVF Conference on Computer Vision and Pattern Recognition (CVPR)*, 2020. 5
- [5] Jinze Bai, Shuai Bai, Yunfei Chu, Zeyu Cui, Kai Dang, Xiaodong Deng, Yang Fan, Wenbin Ge, Yu Han, Fei Huang, et al. Qwen technical report. *arXiv preprint arXiv:2309.16609*, 2023. 5, 8, 9
- [6] Nicolas Carion, Francisco Massa, Gabriel Synnaeve, Nicolas Usunier, Alexander Kirillov, and Sergey Zagoruyko. End-to-end object detection with transformers. In *European conference on computer vision*, pages 213–229. Springer, 2020. 6, 5
- [7] Gongwei Chen, Leyang Shen, Rui Shao, Xiang Deng, and Liqiang Nie. Lion: Empowering multimodal large language model with dual-level visual knowledge. In *Proceedings of the IEEE/CVF Conference on Computer Vision and Pattern Recognition*, pages 26540–26550, 2024. 8, 9
- [8] Jun Chen, Deyao Zhu, Xiaoqian Shen, Xiang Li, Zechun Liu, Pengchuan Zhang, Raghuraman Krishnamoorthi, Vikas Chandra, Yunyang Xiong, and Mohamed Elhoseiny. Minigt-v2: large language model as a unified interface for vision-language multi-task learning. *arXiv preprint arXiv:2310.09478*, 2023. 2, 8, 9
- [9] Keqin Chen, Zhao Zhang, Weili Zeng, Richong Zhang, Feng Zhu, and Rui Zhao. Shikra: Unleashing multimodal llm’s referential dialogue magic. *arXiv preprint arXiv:2306.15195*, 2023. 2, 6, 8, 5, 9
- [10] Yen-Chun Chen, Linjie Li, Licheng Yu, Ahmed El Kholy, Faisal Ahmed, Zhe Gan, Yu Cheng, and Jingjing Liu. Uniter: Universal image-text representation learning. In *European conference on computer vision*, pages 104–120. Springer, 2020. 9
- [11] Zhe Chen, Jiannan Wu, Wenhai Wang, Weijie Su, Guo Chen, Sen Xing, Muyan Zhong, Qinglong Zhang, Xizhou Zhu, Lewei Lu, Bin Li, Ping Luo, Tong Lu, Yu Qiao, and Jifeng Dai. Internvl: Scaling up vision foundation models and aligning for generic visual-linguistic tasks. *arXiv preprint arXiv:2312.14238*, 2023. 5, 8
- [12] Bowen Cheng, Alexander G. Schwing, and Alexander Kirillov. Per-pixel classification is not all you need for semantic segmentation. 2021. 6, 8
- [13] Tianheng Cheng, Lin Song, Yixiao Ge, Wenyu Liu, Xinggang Wang, and Ying Shan. Yolo-world: Real-time open-vocabulary object detection. In *Proceedings of the IEEE/CVF Conference on Computer Vision and Pattern Recognition*, pages 16901–16911, 2024. 3
- [14] Mehdi Cherti, Romain Beaumont, Ross Wightman, Mitchell Wortsman, Gabriel Ilharco, Cade Gordon, Christoph Schuhmann, Ludwig Schmidt, and Jenia Jitsev. Reproducible scaling laws for contrastive language-image learning. In *Proceedings of the IEEE/CVF Conference on Computer Vision and Pattern Recognition*, pages 2818–2829, 2023. 5
- [15] Marius Cordts, Mohamed Omran, Sebastian Ramos, Timo Rehfeld, Markus Enzweiler, Rodrigo Benenson, Uwe Franke, Stefan Roth, and Bernt Schiele. The cityscapes dataset for semantic urban scene understanding. In *Proceedings of the IEEE conference on computer vision and pattern recognition*, pages 3213–3223, 2016. 3, 4, 7
- [16] Wenliang Dai, Junnan Li, Dongxu Li, Anthony Meng Huat Tiong, Junqi Zhao, Weisheng Wang, Boyang Li, Pascale Fung, and Steven Hoi. Instructblip: Towards general-purpose vision-language models with instruction tuning, 2023. 8
- [17] Henghui Ding, Chang Liu, Suchen Wang, and Xudong Jiang. Vision-language transformer and query generation for referring segmentation. In *Proceedings of the IEEE International Conference on Computer Vision*, 2021. 10
- [18] Xiaoyi Dong, Jianmin Bao, Yinglin Zheng, Ting Zhang, Dongdong Chen, Hao Yang, Ming Zeng, Weiming Zhang, Lu Yuan, Dong Chen, et al. Maskclip: Masked self-distillation advances contrastive language-image pretraining. In *Proceedings of the IEEE/CVF Conference on Computer Vision and Pattern Recognition*, pages 10995–11005, 2023. 9
- [19] Hao Fei, Shengqiong Wu, Hanwang Zhang, Tat-Seng Chua, and Shuicheng Yan. Vitron: A unified pixel-level vision llm for understanding, generating, segmenting, editing, 2024. 2, 3, 6, 5, 10
- [20] Zhe Gan, Yen-Chun Chen, Linjie Li, Chen Zhu, Yu Cheng, and Jingjing Liu. Large-scale adversarial training for vision-and-language representation learning. *Advances in Neural Information Processing Systems*, 33:6616–6628, 2020. 9
- [21] Andreas Geiger, Philip Lenz, Christoph Stiller, and Raquel Urtasun. Vision meets robotics: The kitti dataset. *International Journal of Robotics Research (IJRR)*, 2013. 4
- [22] Cristina González, Nicolás Ayobi, Isabela Hernández, José Hernández, Jordi Pont-Tuset, and Pablo Arbeláez. Panoptic narrative grounding. In *Proceedings of the IEEE/CVF International Conference on Computer Vision*, pages 1364–1373, 2021. 4, 7
- [23] Qiushan Guo, Shalini De Mello, Hongxu Yin, Wonmin Byeon, Ka Chun Cheung, Yizhou Yu, Ping Luo, and Sifei Liu. Regionpt: Towards region understanding vision language model. In *Proceedings of the IEEE/CVF Conference on Computer Vision and Pattern Recognition*, pages 13796–13806, 2024. 8
- [24] Aishwarya Kamath, Mannat Singh, Yann LeCun, Gabriel Synnaeve, Ishan Misra, and Nicolas Carion. Mdetr-modulated

- detection for end-to-end multi-modal understanding. In *Proceedings of the IEEE/CVF international conference on computer vision*, pages 1780–1790, 2021. 9
- [25] Sahar Kazemzadeh, Vicente Ordonez, Mark Matten, and Tamara Berg. Referitgame: Referring to objects in photographs of natural scenes. In *Proceedings of the 2014 conference on empirical methods in natural language processing (EMNLP)*, pages 787–798, 2014. 8, 3, 4, 7
- [26] Alexander Kirillov, Eric Mintun, Nikhila Ravi, Hanzi Mao, Chloe Rolland, Laura Gustafson, Tete Xiao, Spencer Whitehead, Alexander C Berg, Wan-Yen Lo, et al. Segment anything. In *Proceedings of the IEEE/CVF International Conference on Computer Vision*, pages 4015–4026, 2023. 3, 6, 8, 9, 5, 7, 10
- [27] Ranjay Krishna, Yuke Zhu, Oliver Groth, Justin Johnson, Kenji Hata, Joshua Kravitz, Stephanie Chen, Yannis Kalantidis, Li-Jia Li, David A Shamma, et al. Visual genome: Connecting language and vision using crowdsourced dense image annotations. *International journal of computer vision*, 123:32–73, 2017. 3, 4, 7
- [28] Xin Lai, Zhuotao Tian, Yukang Chen, Yanwei Li, Yuhui Yuan, Shu Liu, and Jiaya Jia. Lisa: Reasoning segmentation via large language model. In *Proceedings of the IEEE/CVF Conference on Computer Vision and Pattern Recognition*, pages 9579–9589, 2024. 2, 3, 4, 5, 6, 8, 10
- [29] Yifan Li, Yifan Du, Kun Zhou, Jinpeng Wang, Wayne Xin Zhao, and Ji-Rong Wen. Evaluating object hallucination in large vision-language models. *arXiv preprint arXiv:2305.10355*, 2023. 7, 8
- [30] Tsung-Yi Lin, Michael Maire, Serge Belongie, James Hays, Pietro Perona, Deva Ramanan, Piotr Dollár, and C Lawrence Zitnick. Microsoft coco: Common objects in context. In *Computer Vision—ECCV 2014: 13th European Conference, Zurich, Switzerland, September 6–12, 2014, Proceedings, Part V 13*, pages 740–755. Springer, 2014. 3, 4, 7
- [31] Ziyi Lin, Chris Liu, Renrui Zhang, Peng Gao, Longtian Qiu, Han Xiao, Han Qiu, Chen Lin, Wenqi Shao, Keqin Chen, et al. Sphinx: The joint mixing of weights, tasks, and visual embeddings for multi-modal large language models. *arXiv preprint arXiv:2311.07575*, 2023. 2
- [32] Chang Liu, Henghui Ding, and Xudong Jiang. GRES: Generalized referring expression segmentation. In *CVPR*, 2023. 8, 10
- [33] Haotian Liu, Chunyuan Li, Qingyang Wu, and Yong Jae Lee. Visual instruction tuning, 2023. 3, 4, 7
- [34] Haotian Liu, Chunyuan Li, Qingyang Wu, and Yong Jae Lee. Visual instruction tuning. *Advances in neural information processing systems*, 36, 2024. 2, 5, 8
- [35] Shilong Liu, Hao Cheng, Haotian Liu, Hao Zhang, Feng Li, Tianhe Ren, Xueyan Zou, Jianwei Yang, Hang Su, Jun Zhu, et al. Llava-plus: Learning to use tools for creating multimodal agents. *arXiv preprint arXiv:2311.05437*, 2023. 2, 3, 5
- [36] Shilong Liu, Zhaoyang Zeng, Tianhe Ren, Feng Li, Hao Zhang, Jie Yang, Qing Jiang, Chunyuan Li, Jianwei Yang, Hang Su, et al. Grounding dino: Marrying dino with grounded pre-training for open-set object detection. *arXiv preprint arXiv:2303.05499*, 2023. 3, 6, 5, 9
- [37] Gen Luo, Yiyi Zhou, Xiaoshuai Sun, Liujuan Cao, Chenglin Wu, Cheng Deng, and Rongrong Ji. Multi-task collaborative network for joint referring expression comprehension and segmentation. In *Proceedings of the IEEE/CVF Conference on Computer Vision and Pattern Recognition (CVPR)*, 2020. 10
- [38] Chuofan Ma, Yi Jiang, Jiannan Wu, Zehuan Yuan, and Xiaojuan Qi. Groma: Localized visual tokenization for grounding multimodal large language models. *arXiv preprint arXiv:2404.13013*, 2024. 8
- [39] Kenneth Marino, Mohammad Rastegari, Ali Farhadi, and Roozbeh Mottaghi. Ok-vqa: A visual question answering benchmark requiring external knowledge. In *Proceedings of the IEEE/cvf conference on computer vision and pattern recognition*, pages 3195–3204, 2019. 7
- [40] Pushmeet Kohli Nathan Silberman, Derek Hoiem and Rob Fergus. Indoor segmentation and support inference from rgb-d images. In *ECCV*, 2012. 4
- [41] Zhiliang Peng, Wenhui Wang, Li Dong, Yaru Hao, Shaohan Huang, Shuming Ma, and Furu Wei. Kosmos-2: Grounding multimodal large language models to the world. *arXiv preprint arXiv:2306.14824*, 2023. 2, 3, 8, 4, 7, 9
- [42] Bryan A Plummer, Liwei Wang, Chris M Cervantes, Juan C Caicedo, Julia Hockenmaier, and Svetlana Lazebnik. Flickr30k entities: Collecting region-to-phrase correspondences for richer image-to-sentence models. In *Proceedings of the IEEE international conference on computer vision*, pages 2641–2649, 2015. 7, 8, 4
- [43] Shraman Pramanick, Guangxing Han, Rui Hou, Sayan Nag, Ser-Nam Lim, Nicolas Ballas, Qifan Wang, Rama Chellappa, and Amjad Almahairi. Jack of all tasks master of many: Designing general-purpose coarse-to-fine vision-language model. In *Proceedings of the IEEE/CVF Conference on Computer Vision and Pattern Recognition*, pages 14076–14088, 2024. 9
- [44] Alec Radford, Jong Wook Kim, Chris Hallacy, Aditya Ramesh, Gabriel Goh, Sandhini Agarwal, Girish Sastry, Amanda Askell, Pamela Mishkin, Jack Clark, et al. Learning transferable visual models from natural language supervision. In *International conference on machine learning*, pages 8748–8763. PMLR, 2021. 5
- [45] Hanoona Rasheed, Muhammad Maaz, Sahal Shaji, Abdelrahman Shaker, Salman Khan, Hisham Cholakkal, Rao M Anwer, Eric Xing, Ming-Hsuan Yang, and Fahad S Khan. Glamm: Pixel grounding large multimodal model. In *Proceedings of the IEEE/CVF Conference on Computer Vision and Pattern Recognition*, pages 13009–13018, 2024. 2, 3, 4, 5, 6, 8, 7, 10
- [46] Zhongwei Ren, Zhicheng Huang, Yunchao Wei, Yao Zhao, Dongmei Fu, Jiashi Feng, and Xiaojie Jin. Pixellm: Pixel reasoning with large multimodal model. In *Proceedings of the IEEE/CVF Conference on Computer Vision and Pattern Recognition*, pages 26374–26383, 2024. 4, 5, 6, 7, 8, 10
- [47] Christoph Schuhmann, Romain Beaumont, Richard Vencu, Cade Gordon, Ross Wightman, Mehdi Cherti, Theo Coombes, Aarush Katta, Clayton Mullis, Mitchell Wortsman, et al. Laion-5b: An open large-scale dataset for training next generation image-text models. *Advances in Neural Information Processing Systems*, 35:25278–25294, 2022. 3

- [48] Yongliang Shen, Kaitao Song, Xu Tan, Dongsheng Li, Weiming Lu, and Yueting Zhuang. Hugginggpt: Solving ai tasks with chatgpt and its friends in hugging face. *Advances in Neural Information Processing Systems*, 36, 2024. 2
- [49] Shweta Singh, Aayan Yadav, Jitesh Jain, Humphrey Shi, Justin Johnson, and Karan Desai. Benchmarking object detectors with coco: A new path forward, 2024. 3, 4, 7
- [50] Yan Tai, Weichen Fan, Zhao Zhang, and Ziwei Liu. Link-context learning for multimodal llms. In *Proceedings of the IEEE/CVF Conference on Computer Vision and Pattern Recognition*, pages 27176–27185, 2024. 2, 4
- [51] Peng Wang, An Yang, Rui Men, Junyang Lin, Shuai Bai, Zhikang Li, Jianxin Ma, Chang Zhou, Jingren Zhou, and Hongxia Yang. Ofa: Unifying architectures, tasks, and modalities through a simple sequence-to-sequence learning framework. In *International conference on machine learning*, pages 23318–23340. PMLR, 2022. 9
- [52] Wenhai Wang, Zhe Chen, Xiaokang Chen, Jiannan Wu, Xizhou Zhu, Gang Zeng, Ping Luo, Tong Lu, Jie Zhou, Yu Qiao, and Jifeng Dai. Visionllm: Large language model is also an open-ended decoder for vision-centric tasks. In *Advances in Neural Information Processing Systems 36: Annual Conference on Neural Information Processing Systems 2023, NeurIPS 2023, New Orleans, LA, USA, December 10 - 16, 2023*, 2023. 2
- [53] Weiyun Wang, Min Shi, Qingyun Li, Wenhai Wang, Zhenhang Huang, Linjie Xing, Zhe Chen, Hao Li, Xizhou Zhu, Zhiguo Cao, et al. The all-seeing project: Towards panoptic visual recognition and understanding of the open world. *arXiv preprint arXiv:2308.01907*, 2023. 8
- [54] Chenfei Wu, Shengming Yin, Weizhen Qi, Xiaodong Wang, Zecheng Tang, and Nan Duan. Visual chatgpt: Talking, drawing and editing with visual foundation models. *CoRR*, abs/2303.04671, 2023. 2
- [55] Junfeng Wu, Yi Jiang, Qihao Liu, Zehuan Yuan, Xiang Bai, and Song Bai. General object foundation model for images and videos at scale. In *Proceedings of the IEEE/CVF Conference on Computer Vision and Pattern Recognition*, pages 3783–3795, 2024. 10
- [56] Jiannan Wu, Muyan Zhong, Sen Xing, Zeqiang Lai, Zhaoyang Liu, Wenhai Wang, Zhe Chen, Xizhou Zhu, Lewei Lu, Tong Lu, Ping Luo, Yu Qiao, and Jifeng Dai. Visionllm v2: An end-to-end generalist multimodal large language model for hundreds of vision-language tasks. *CoRR*, abs/2406.08394, 2024. 2, 3, 4, 5, 6, 7, 8, 9, 1, 10
- [57] Jialian Wu, Jianfeng Wang, Zhengyuan Yang, Zhe Gan, Zicheng Liu, Junsong Yuan, and Lijuan Wang. Grit: A generative region-to-text transformer for object understanding. In *European Conference on Computer Vision*, pages 207–224. Springer, 2025. 8
- [58] Size Wu, Sheng Jin, Wenwei Zhang, Lumin Xu, Wentao Liu, Wei Li, and Chen Change Loy. F-Imm: Grounding frozen large multimodal models. *arXiv preprint arXiv:2406.05821*, 2024. 2, 8
- [59] Ke Xian, Jianming Zhang, Oliver Wang, Long Mai, Zhe Lin, and Zhiguo Cao. Structure-guided ranking loss for single image depth prediction. In *Proceedings of the IEEE/CVF Conference on Computer Vision and Pattern Recognition*, pages 611–620, 2020. 4
- [60] Jiarui Xu, Sifei Liu, Arash Vahdat, Wonmin Byeon, Xiaolong Wang, and Shalini De Mello. Open-Vocabulary Panoptic Segmentation with Text-to-Image Diffusion Models. *arXiv preprint arXiv:2303.04803*, 2023. 9
- [61] Jiarui Xu, Xingyi Zhou, Shen Yan, Xiuye Gu, Anurag Arnab, Chen Sun, Xiaolong Wang, and Cordelia Schmid. Pixel-aligned language model. In *Proceedings of the IEEE/CVF Conference on Computer Vision and Pattern Recognition*, pages 13030–13039, 2024. 2, 8, 7, 10
- [62] Mengde Xu, Zheng Zhang, Fangyu Wei, Han Hu, and Xiang Bai. San: Side adapter network for open-vocabulary semantic segmentation. *IEEE Transactions on Pattern Analysis and Machine Intelligence*, 2023. 9
- [63] Bin Yan, Yi Jiang, Jiannan Wu, Dong Wang, Ping Luo, Zehuan Yuan, and Huchuan Lu. Universal instance perception as object discovery and retrieval. In *Proceedings of the IEEE/CVF Conference on Computer Vision and Pattern Recognition*, pages 15325–15336, 2023. 10
- [64] Zhengyuan Yang, Linjie Li, Jianfeng Wang, Kevin Lin, Ehsan Azarnasab, Faisal Ahmed, Zicheng Liu, Ce Liu, Michael Zeng, and Lijuan Wang. Mm-react: Prompting chatgpt for multimodal reasoning and action. *arXiv preprint arXiv:2303.11381*, 2023. 2
- [65] Qinghao Ye, Haiyang Xu, Guohai Xu, Jiabo Ye, Ming Yan, Yiyang Zhou, Junyang Wang, Anwen Hu, Pengcheng Shi, Yaya Shi, et al. mplug-owl: Modularization empowers large language models with multimodality. *arXiv preprint arXiv:2304.14178*, 2023. 8
- [66] Haoxuan You, Haotian Zhang, Zhe Gan, Xianzhi Du, Bowen Zhang, Zirui Wang, Liangliang Cao, Shih-Fu Chang, and Yinfei Yang. Ferret: Refer and ground anything anywhere at any granularity. *arXiv preprint arXiv:2310.07704*, 2023. 2, 8, 9
- [67] Licheng Yu, Zhe Lin, Xiaohui Shen, Jimei Yang, Xin Lu, Mohit Bansal, and Tamara L Berg. Mattnet: Modular attention network for referring expression comprehension. In *Proceedings of the IEEE conference on computer vision and pattern recognition*, pages 1307–1315, 2018. 9
- [68] Yuqian Yuan, Wentong Li, Jian Liu, Dongqi Tang, Xinjie Luo, Chi Qin, Lei Zhang, and Jianke Zhu. Osprey: Pixel understanding with visual instruction tuning. In *Proceedings of the IEEE/CVF Conference on Computer Vision and Pattern Recognition*, pages 28202–28211, 2024. 2, 5, 6, 8, 3, 4, 7, 10
- [69] Rowan Zellers, Yonatan Bisk, Ali Farhadi, and Yejin Choi. From recognition to cognition: Visual commonsense reasoning. In *The IEEE Conference on Computer Vision and Pattern Recognition (CVPR)*, 2019. 4, 7
- [70] Ao Zhang, Liming Zhao, Chen-Wei Xie, Yun Zheng, Wei Ji, and Tat-Seng Chua. Next-chat: An lmm for chat, detection and segmentation. *arXiv preprint arXiv:2311.04498*, 2023. 2, 9, 10
- [71] Hao Zhang, Hongyang Li, Feng Li, Tianhe Ren, Xueyan Zou, Shilong Liu, Shijia Huang, Jianfeng Gao, Lei Zhang, Chunyuan Li, et al. Llava-grounding: Grounded visual chat with large multimodal models. *arXiv preprint arXiv:2312.02949*, 1, 2023. 4, 7

- [72] Yichi Zhang, Ziqiao Ma, Xiaofeng Gao, Suhaila Shakiah, Qiaozi Gao, and Joyce Chai. Groundhog: Grounding large language models to holistic segmentation. In *Proceedings of the IEEE/CVF conference on computer vision and pattern recognition*, pages 14227–14238, 2024. [2](#), [8](#), [10](#)
- [73] Zheng Zhang, Yeyao Ma, Enming Zhang, and Xiang Bai. Psalm: Pixelwise segmentation with large multi-modal model. *arXiv preprint arXiv:2403.14598*, 2024. [2](#), [3](#), [5](#), [8](#), [9](#), [4](#), [7](#), [10](#)
- [74] Yang Zhao, Zhijie Lin, Daquan Zhou, Zilong Huang, Jiashi Feng, and Bingyi Kang. Bubogpt: Enabling visual grounding in multi-modal llms. *arXiv preprint arXiv:2307.08581*, 2023. [2](#), [8](#)
- [75] Lianmin Zheng, Wei-Lin Chiang, Ying Sheng, Siyuan Zhuang, Zhanghao Wu, Yonghao Zhuang, Zi Lin, Zhuohan Li, Dacheng Li, Eric Xing, et al. Judging llm-as-a-judge with mt-bench and chatbot arena. *Advances in Neural Information Processing Systems*, 36:46595–46623, 2023. [5](#)
- [76] Bolei Zhou, Hang Zhao, Xavier Puig, Sanja Fidler, Adela Barriuso, and Antonio Torralba. Scene parsing through ade20k dataset. In *Proceedings of the IEEE conference on computer vision and pattern recognition*, pages 633–641, 2017. [3](#), [4](#), [7](#)
- [77] Zijian Zhou, Zheng Zhu, Holger Caesar, and Miaoqing Shi. Openspg: Open-set panoptic scene graph generation via large multimodal models. *arXiv preprint arXiv:2407.11213*, 2024. [4](#), [7](#)
- [78] Yuke Zhu, Oliver Groth, Michael Bernstein, and Li Fei-Fei. Visual7w: Grounded question answering in images. In *Proceedings of the IEEE conference on computer vision and pattern recognition*, pages 4995–5004, 2016. [4](#), [7](#)
- [79] Xueyan Zou*, Zi-Yi Dou*, Jianwei Yang*, Zhe Gan, Linjie Li, Chunyuan Li, Xiyang Dai, Jianfeng Wang, Lu Yuan, Nanyun Peng, Lijuan Wang, Yong Jae Lee*, and Jianfeng Gao*. Generalized decoding for pixel, image and language. 2022. [10](#)
- [80] Xueyan Zou, Jianwei Yang, Hao Zhang, Feng Li, Linjie Li, Jianfeng Wang, Lijuan Wang, Jianfeng Gao, and Yong Jae Lee. Segment everything everywhere all at once. *Advances in Neural Information Processing Systems*, 36, 2024. [9](#), [10](#)

REF-VLM: Triplet-Based Referring Paradigm for Unified Visual Decoding

Supplementary Material

Contents

1. Introduction	2
2. Related Works	3
3. Unified Instruction Pipeline	3
3.1. Triplet-Based Referring Paradigm	3
3.2. Visual Decoding Chain-of-Thought	4
3.3. Visual-Task Instruction Following Dataset . .	5
4. End-to-End Decoding Framework	5
4.1. Unified Training Workflow	5
4.2. Mask-Guided Aggregation	6
4.3. Visual Unit Decoders	6
5. Experiments	7
5.1. Quantitative Results	7
5.2. Ablation Study	9
6. Limitations and Conclusion	9
A. VD-CoT Details	1
B. VT-Instruct Construction	3
B.1. Definition of Each Downstream Task	3
B.2. Dataset Construction Details	3
C. Implementation Details	5
C.1. Group Hungarian Matcher	5
C.2. Extend to More Plugins	5
D. Training Details	5
E. Freeform Open-Vocabulary Identification	8
E.1. Task Definition	8
E.2. mAP Similarity (mAP _S)	8
F. More Results	8
F.1. More Experimental Results	8
F.2. More Ablation Results	10
G. More Visualization Results	11

A. VD-CoT Details

In this section, we provide additional details about VD-CoT, including its functionality, design rationale, and advantages over existing approaches.

Unified Instruction Tuning for Visual Decoding Tasks

As mentioned in Section 3.2, classical approaches based on learnable queries typically require the model to provide an additional special token (referred to as `<REF>` in our setting) for each visual entity (referred to as `Phrase` in our setting). This token is used to represent the visual entity and serves as a learnable query for downstream task decoders. However, in the vanilla `Phrase + <REF>` approach, although the `<REF>` may have a length greater than 1, it always refers to the same instance and decodes into a single target. This design limits the flexibility of instruction-tuning methods, when the instance represented by the phrase has multiple occurrences, this approach fails to adapt effectively. For example, the Decoding Triplets process in VD-CoT supports both “one-to-one” decoding (e.g., “There are two capybaras, `<Phrase>a big one</Phrase>`[0]`<REF>` and `<Phrase>a small one</Phrase>`[0]`<REF>`.”) and “one-to-many” decoding (e.g., “There are `<Phrase>two capybaras</Phrase>`[0]`<REF>`[1]`<REF>`.”), where all content enclosed in angle brackets represents special tokens. All special token definitions can be found in Table 10, and the VD-CoT processes for different tasks are detailed in Appendix F.

Decoding Triplets for Prevent Task Conflicts In visual multi-task training schemes for MLLMs, task conflict is typically mitigated by introducing different special tokens for each task. For instance, VisionLLM v2 [56] incorporates eight distinct special tokens. However, as the number of tasks increases, the required special tokens also grow, and introducing each new token necessitates retraining the MLLM.

In our VD-CoT, we employ the `<REF>` token to refer to visual entities for any task. To prevent potential task conflicts, we leverage the next-token prediction mechanism of MLLMs. Before generating the `<REF>` token, the model is required to first output the decoding unit of the current task, forming “`Phrase-Unit-<REF>`” triplets. As shown in Figure 5, the two curves represent the response magnitudes of two `<REF>` tokens to the MLLM’s answers, with the shaded regions indicating unit contents. During the generation process, `<REF>` exhibits a high response to the `Unit`,

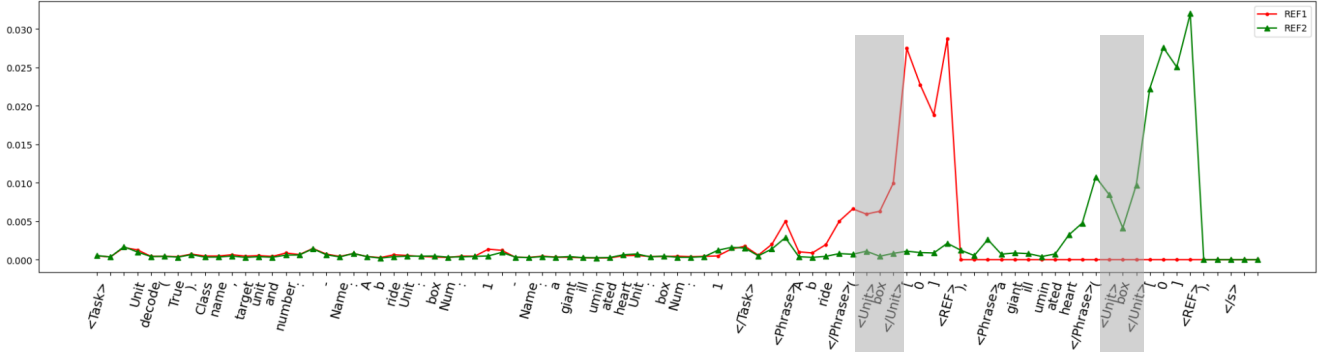


Figure 5. **Attention Significance of <REF> Tokens for MLLM Output Tokens.** We selected a general segmentation task with the prompt “please segment objects in the image <image>.” The model outputs two classification results: “a bride” and “a giant illuminated heart”, using our designed VD-CoT format. We used attention visualization techniques to generate attention significance maps for the REF token with respect to each output token of the MLLM. The attention values from each layer were averaged and visualized, as shown in the figure above. The figure demonstrates that each <REF> token exhibits high attention response values to the preceding <Phrase>, <Unit>, and output numbers.

Table 10. **Special token lists for training REF-VLM.** During REF-VLM training, the special tokens mentioned above are predefined and added to the LLM’s vocabulary for training.

Speical Token Lists	Token Names	Speical Token Lists	Token Names
Visual Prompt Token	[VPT]	Begin of Task Token	<Task>
Visual Reference Token	<REF>	End of Task Token	</Task>
Phrase Start	<Phrase>	Begin of Unit Token	<Unit>
Phrase End	</Phrase>	End of Unit Token	</Unit>
Default Pad Token	[PAD]	Image Placeholder	<image>

ensuring that the representation of <REF> varies across tasks, thereby avoiding task conflicts.

Link-Context Learning for Unknown Tasks Link-Context Learning (LCL) [50] enables MLLMs to acquire the knowledge required for unknown tasks from few-shot prompts. In our VD-CoT setting, since the MLLM acts as a router and outputs the type of decoding content in textual form, we can leverage LCL to handle unknown tasks that do not appear in the training set using a few-shot approach.

Specifically, we augment the instruction-tuning data with random samples where user inputs are matched with Unit decoding. For example, the input prompts include “You are performing a new task, the unit of the task is [unit name], please [task-specific command]”, and in the corresponding answer, the unit name is replaced with the content from the prompt. Through this approach, VD-CoT requires the MLLM to determine the current decoding task based on the input prompt and form the corresponding triplets, eliminating the need to introduce a new special token for each task. This provides REF-VLM with incremental learning capabilities.

VD-CoT for High-Accuracy Triplets REF-VLM supports a wide range of visual decoding tasks, with differences in how “Phrase-Unit-<REF>” triplets are constructed for each task. Complex instruction-tuning schemes can lead to reduced generation accuracy by the MLLM. For instance, in the “one-to-many” decoding setting, the <REF> token may fail to match the expected number of instances in the image, instead entering an infinite generation loop. Similarly, incorrect unit predictions for the current task can degrade the decoding performance of the <REF> token.

In the first step of VD-CoT, the MLLM performs step-by-step reasoning over the image, including identifying the visual entities, decoding type, and number of instances. During the Decoding Triplets step, since the necessary decoding information has already been established, the triplets are organized according to a predefined paradigm, improving the accuracy of the generated content. As shown in Table 9, the introduction of VD-CoT significantly enhances the model’s reasoning accuracy.

B. VT-Instruct Construction

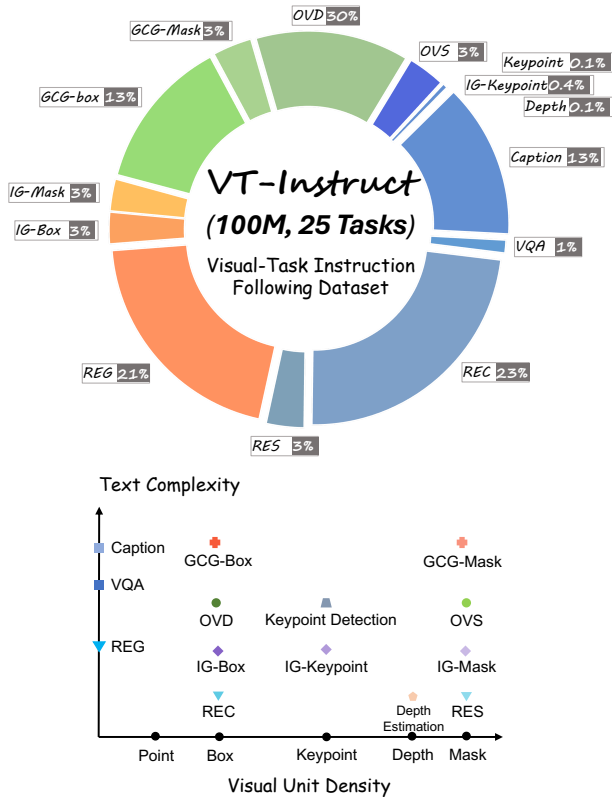


Figure 6. **Data Distribution Map.** VT-Instruct comprises four output units—box, keypoint, depth, and mask—paired with either low (phrases) or high (sentences) text complexity, with different visual prompts unified under the same task for clarity.

B.1. Definition of Each Downstream Task

VT-Instruct includes 7 different downstream tasks, as shown in Figure 7. The Visual Understanding task includes Image Captioning and Visual Question Answering (VQA), involving image-text inputs and text-only outputs. Referring Expression tasks cover Referring Expression Comprehension (REC), Referring Expression Segmentation (RES), and Referring Expression Generation (REG). While REC and RES require models to predict bounding boxes or masks in response to a query about a specific region in an image, REG involves generating descriptive text from visual inputs like points, boxes, scribbles, or masks. Interactive Grounding (IG) enables users to provide prompts via both text and interactive inputs (e.g., points, boxes, masks), allowing MLLMs to interpret and generate corresponding outputs. Open-Vocabulary Identification focuses on localizing and segmenting objects from descriptive text, even if the object categories were not part of the training data. For traditional Open-Vocabulary tasks performed by current MLLM, it typ-

ically requires user inputs specific class names, Grounded Conversation Generation (GCG) produces natural language responses interwoven with bounding boxes or masks, with the GCG task further divided into GCG-box (bounding box outputs) and GCG-mask (mask outputs).

B.2. Dataset Construction Details

For each task, we select a unique prompt-unit pair to develop task-specific instructions. For example, visual understanding task encompasses Image Captioning and Visual Question Answering (VQA), with image-text inputs and pure text outputs. To facilitate MLLMs in comprehending image-level information and addressing diverse questions, we construct conversations for visual understanding tasks using our proposed pipeline with the COCO [30], Grand [45], GRIT [41], VQAv2 [3], and LLaVA-instruct [33] datasets, which collectively comprise over 15 million image-text pairs featuring multi-turn conversations. Referring expression tasks include Referring Expression Comprehension (REC), Referring Expression Segmentation (RES), and Referring Expression Generation (REG). The REC and RES tasks require the model to respond to a question or description regarding a specific area in an image, predicting bounding boxes or masks. In contrast, the REG task involves inputs such as points, boxes, scribbles, and masks, with the model expected to generate a descriptive response based on the visual prompts. We construct conversations for referring expression task from refCOCO [25], refCOCO+ [25], refCOCOg [25], Grand [45], GRIT [30], Osprey [68], Visual Genome [27] datasets with more than 22 million samples. Interactive grounding allows users to provide prompts through both text and interactive elements, such as points, boxes, masks, or scribbles, enabling MLLMs to interpret these inputs and generate corresponding outputs, including bounding boxes or masks. We constructed interactive grounding samples using the COCO-interactive [73] dataset, which contains over 64 million examples. The open-vocabulary identification task focuses on localizing and segmenting objects in an image based on descriptive text prompts, even if the specific object categories were not included in the model’s training data. To equip REF-VLM with zero-shot capabilities for object detection and segmentation—similar to traditional open-vocabulary detection models (e.g., YOLO-World [13]) and segmentation models (e.g., SAM [26])—we designed a multimodal conversation system using bounding boxes and masks annotations from the GRIT [41], Grand [45], COCO-REM [49], ADE20k [76], and Cityscapes [15] datasets, resulting in a corpus of over 20 million examples. Grounded conversation generation (GCG) aims to produce natural language responses interwoven with bounding boxes or object segmentation masks. The GCG task is divided into GCG-box, which outputs bounding boxes, and GCG-mask, which outputs masks. We developed these tasks using datasets that

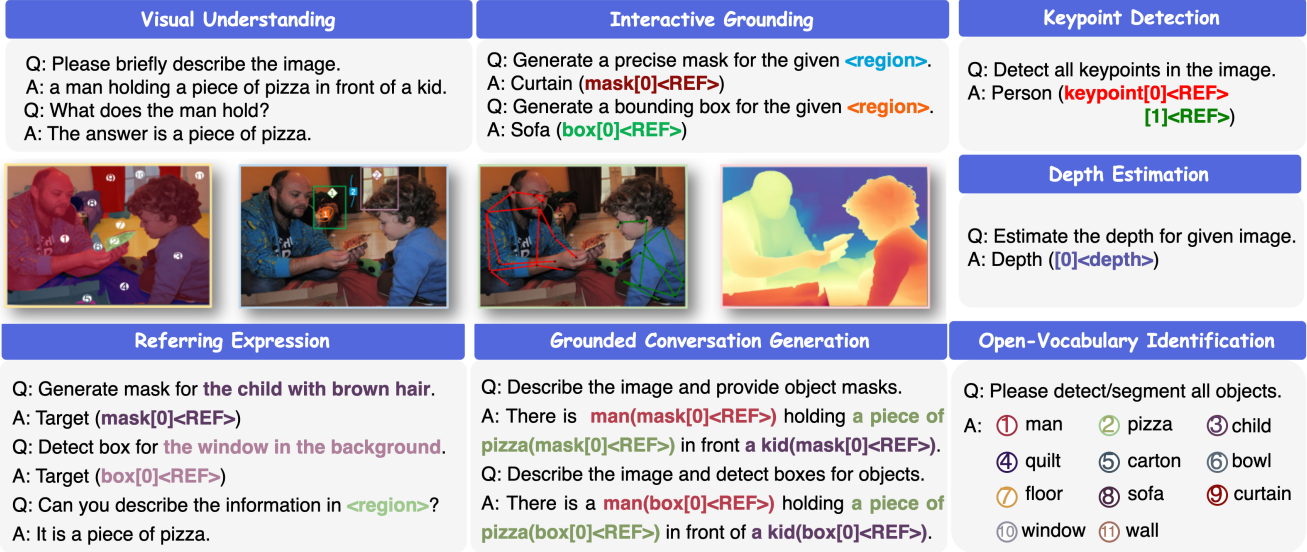


Figure 7. **Example of VT-Instruct Dataset by Using the Automated Data Construction Pipeline.** Our VT-Instruct dataset contains seven distinct downstream tasks, including Visual Understanding, Referring Expression, Interactive Grounding, Grounded Conversation Generation, Open-Vocabulary Identification and Depth Estimation.

Table 11. **Data statistics of VT-Instruct and actual use of dataset in the training process.** Multiple datasets were utilized to train REF-VLM, with some supporting multiple tasks. For instance, Grand [45] enables tasks such as captioning, REC, RES, REG, GCG, and open-vocabulary identification. Most datasets within VT-Instruct were employed as subsets in our training process.

Task	Sub-Task	Original Dataset	Construction Number	Actual Use
Visual Understanding	Caption	COCO [30], Grand [45], GRIT [41]	15,980,000	780,000
	VQA	VQAv2 [3], LLaVA-Instruct [33], VCR [69]	1,310,000	1,310,000
Referring Expression	REC	RefCOCO [25], RefCOCO+ [25], RefCOCOg [25], Grand [45], GRIT [41]	22,880,000	880,000
	RES	RefCOCO [25], RefCOCO+ [25], RefCOCOg [25], Grand [45]	3,880,000	680,000
	REG	RefCOCO [25], RefCOCO+ [25], RefCOCOg [25], Grand [45], GRIT [41], COCO-Interactive [73], Osprey [68], Visual Genome [27], Visual7W [78]	22,750,000	1,200,000
Interactive Grounding	IG-Box	COCO-Interactive [73]	3,200,000	120,000
	IG-Mask	COCO-Interactive [73]	3,200,000	120,000
	IG-Keypoint	COCO [30]	500,000	140,000
Grounded Conversation Generation	GCG-box	GRIT [41], Grand [45], Flickr30k-Entities [42]	15,630,000	540,000
	GCG-mask	Grand [45], LLaVA-Grounding [71], PNG [22], OpenPSG [77]	4,000,000	450,000
Open-Vocabulary Identification	OVD/FOVD	Grand [45], GRIT [41], COCO-REM [49]	15,770,000	600,000
	OVS/FOVS	Grand [45], COCO-REM [49], ADE20k [76], Cityscapes [15]	3,795,000	600,000
Keypoint Detection	-	COCO [30]	140,000	140,000
Depth Estimation	-	Kitti [21], HRWSI [59], NYU [40]	150,000	-

include captions and phrases associated with bounding box or mask annotations, such as Flickr30k-entities [42], Grand [45], GRIT [41], LLaVA-grounding [71], OpenPSG [77], and PNG [22], collectively comprising over 18 million annotations. The example of our dataset can be seen in Figure 7. The total distribution and overall statistics of our dataset can

be seen in Figure 6 and Table 11.

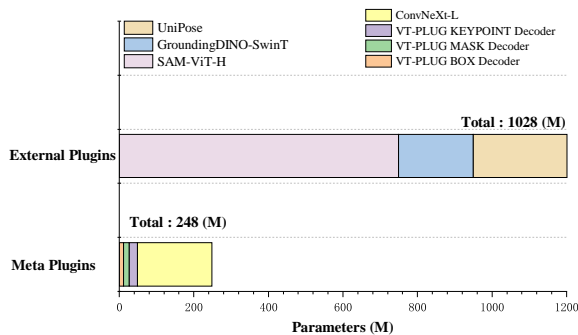


Figure 8. **The Comparison of parameter numbers.** Our Meta-plugins uses 248M parameters, while the External plugins method requires 1028M.

C. Implementation Details

C.1. Group Hungarian Matcher

Hungarian Matcher DETR [6] uses a combined cost function to compute the matching cost between predictions and targets. This cost function includes:

1. **Box loss:** A measure of the similarity between predicted and target bounding boxes, typically using GIoU or L1 distance.
2. **Classification loss:** The cross-entropy loss between the predicted class distribution and the true class labels.

The Hungarian algorithm always produces exactly M matching pairs, corresponding to the ground truth targets because:

- The algorithm is designed to match all target boxes to predictions.
- If there are more predictions ($N > M$), the algorithm will match the remaining $N - M$ predictions to the “no-object” class.

Thus, the number of matching pairs is always equal to the number of target boxes M . Extra predictions are treated as “no-object” and are not counted in the matching pairs.

Group Hungarian Matcher All visual unit decoding plugins in REF-VLM are built on the DETR architecture and benefit from the `Phrase-Unit-<REF>` triplets structure. Each `<REF>` token uniquely corresponds to a specific phrase and unit, ensuring consistency between visual entity recognition and the visual unit decoding process.

In a “`Phrase-Unit-<REF>`” triplet (the number of `<REF>` token may be greater than 1), the `Phrase` represents the category of the `<REF>` tokens within the group, so there is no need to consider classifying instances (e.g., boxes, masks, etc.) during the decoding process of the reference tokens. In visual decoding tasks, the number of `<REF>` tokens

generated by the MLLM in the answer is strictly equal to the number of target instances. When the number of predictions N equals the number of targets M , the result of the Hungarian Matcher is a perfect match, meaning each prediction is paired with a unique target. Therefore, we group all `<REF>` according to different triplets, perform Hungarian matching within each group, and ultimately obtain a one-to-one matching result to calculate the loss.

C.2. Extend to More Plugins

Our model offers high customizability and scalability. It not only supports the use of custom-designed meta plugins as downstream visual decoders to handle dense prediction tasks but also allows integration with existing pre-trained models by loading their weights and fine-tuning with the VT-Instruct dataset to perform a variety of vision tasks. Additionally, compared to agent-based MLLMs [19, 35], our model is an end-to-end system, enabling end-to-end training and fine-tuning. In our design of the model, we not only design meta plugins, but also replace our meta plugins with pretrained models such as SAM [26], GroundingDINO [36] and UniPose [4] as detailed in Table 12. Additionally, to train these visual decoders simultaneously, we introduce a multimodal, multi-task training paradigm that ensures a consistent computational graph across backward passes when heterogeneous input data from multiple tasks are directed to different decoders. During each forward pass, we construct so-called “fake tensors,” which are essentially null inputs directed to inactive decoders. This approach ensures that every decoder shares the same computational graph, effectively preventing hang-ups during multi-task training. The overall loss of our model mainly come from two components: cross entropy loss from LLM (denoted as \mathcal{L}_{LLM}) and visual decoder loss from each specific downstream decoder (denoted as $\mathcal{L}_{Decoder}$). The overall loss is (λ is the hyperparameter for each loss.):

$$\mathcal{L}_{REF-VLM} = \lambda_0 \mathcal{L}_{LLM} + \sum_{i=1}^n \lambda_i \mathcal{L}_{Decoder_i}. \quad (9)$$

D. Training Details

The training process of REF-VLM is conducted in three stages, during which both CLIP-ViT and CLIP-ConvNeXt are frozen, with no parameter updates. We use eight NVIDIA A800-80GB GPUs in all of our training processes and pick Vicuna-7B as our LLM, CLIP-large-14-336 and CLIP-ConvNeXt-512 as our visual encoder. The details parameters and datasets of each stage is shown in Table 14 and Table 15.

Stage 1. In the first stage, we train the projector to equip the LLM with the capability to understand visual information. REF-VLM adopts the same setup as Shikra [9], freezing all model parameters except for the projector to focus

Table 12. **Implementation Details of Each Component in REF-VLM.** We provide a detailed overview of all components used in REF-VLM’s actual training, including visual encoders, the LLM, the VPT encoder, and visual decoders. Here, “visual decoders (meta)” refers to custom-built decoder architectures, while “visual decoders (model)” refers to existing pretrained architectures. The column “weight init” specifies the initialization method: scratch indicates that the component is trained from scratch, and pretrained indicates that the component is initialized with pretrained weights.

Modules	Weight Init	Config
Visual Encoder	pretrained	CLIP-ViT-L CLIP-ConvNeXt-L
VPT Encoder	scratch	strategy='pooling' patch size=8 num patches=9 use mask token=True use projector=True
Projector	scratch	depth=2 bias=True activation='gelu' output dim=4096
LLM	pretrained	Vicuna-1.5-7B
Box Decoder (Meta)	scratch	use group matcher=True num queries=100 queries input dim=4096 encoder input index=[0,1,2,4] decoder layers=6 d model=256 dropout=0.1 bbox loss coef = 5 giou loss coef=2
Box Decoder (GroundingDINOv2)	pretrained	weight='dino_swint_ogc'
Mask Decoder (Meta)	scratch	use group matcher=True num queries=30 queries input dim=4096 encoder input index=[0,1,2,4] decoder layers=6 d model=256 dropout=0.1 fpn feature size=256 mask feature size=256 mask loss coef=20 dice loss coef=1
Mask Decoder (SAM)	pretrained	weight='sam_vit_l'
Keypoint Decoder (Meta)	scratch	num queries=100 decoder layers=6 d model=256 dropout=0.1 num body points=17 aux loss coef=0.5 cls loss coef=2 cls loss coef=1
Keypoint Decoder (UniPose)	pretrained	weight='unipose_swin_t'

on aligning multimodal data. This stage primarily involves training on visual understanding tasks, such as image captioning and VQA, to improve the projector’s performance in

visual-text alignment. For object detection tasks like REC and GCG-box, we did not incorporate specific downstream visual decoders at this stage. Instead, following the approach in [9], we treated these numeric box inputs as strings to provide the model with a sense of spatial awareness. The first stage was trained for approximately two days with a learning rate of $1e - 5$ using the AdamW optimizer on 64 A800 GPUs, with a batch size of 16 per GPU.

Stage 2. In the second stage, We train a fundamental MLLM combined with different visual plugins. We introduce VPT encoder as our encoder visual plugin, box decoder and mask decoder as our decoder visual plugin. REF-VLM is trained using the VT-Instruct data that we constructed as shown in Section 3.3, updating parameters for all modules except the keypoint decoder. The goal of this stage is to train the LLM and various visual plugins using large-scale data, while the keypoint decoder is excluded from training due to its strong correlation with the box decoder. In this stage, we jointly trained both the encoder and decoder visual plugins to enable the REF-VLM has the ability of predicting boxes and masks with different types of interactive inputs to perform various kinds of downstream tasks. For the VPT encoder, we randomly initialize its parameters and train it together with the LLM and decoder. Additionally, we use a projector to align the output dimensions of the VPT encoder with the input dimensions of the LLM. The parameters of this projector are shared with the projector used between the visual encoder and the LLM. For the box decoder and mask decoder, we applied DETR-like architecture for box decoder and MaskFormer-like architecture for mask decoder. We trained all these decoders from scratch without using pretrained models, as we aimed to ensure greater cohesiveness in our model. This approach allows for the use of a unified visual encoder, making deployment more convenient and avoiding excessive computational overhead. We set the learning rate to $2e - 6$ in the second stage and trained the model on A800 GPUs with a batch size of 16 per GPU for about 9 days.

Stage 3. In the third stage, we train additional visual plugins based on our pretrained foundational MLLM from stage 2 to demonstrate the extensibility of our REF-VLM. During this stage, REF-VLM continued training on the VT-Instruct dataset, updating all modules with newly appended keypoint decoder. The keypoint decoder was initialized with the weights of the box decoder from the second stage. We set the learning rate to $2e - 5$ and trained the keypoint decoder for 5 epochs, which took approximately 10 hours using a batch size of 16 per GPU.

Furthermore, after completing all training processes, we replaced the box decoder with GroundingDINO, the mask decoder with SAM, and the keypoint decoder with UniPose. We then repeated the stage 3 training process to finetune the entire MLLM along with the newly integrated visual

Table 13. **Comparison of different plugin backbones without decoders.** We compared PixelLM [61], GLaMM [45], VisionLLMv2 [56], and our REF-VLM in terms of the parameter count of the backbone used for feature extraction in the visual decoder module and whether it is frozen during training. The backbone refers to the image encoder and prompt encoder components within the model’s decoder module. “Freeze backbone” indicates whether this module’s parameters are frozen during the training process of the entire MLLM.

Model	PixelLM [46]	GLaMM [45]	VisionLLMv2 [56]	REF-VLM
Visual Backbone	CLIP-ViT-H	SAM-ViT-L	DINOSwin-T+UniPoseSwin-T	ConvNeXt-L
Backbone Parameters (M)	986M	308M	319M	199M
Total Parameters (M)	1006M	312M	387M	248M
Freeze Backbone	True	False	False	True

Table 14. **Training details of REF-VLM in 3 stages.** For input resolution, 336 means the input resolution for CLIP-ViT is 336×336 , $336+512$ means the input resolution for CLIP-ViT is 336×336 , and the input resolution for CLIP-ConvNeXt is 512×512 . In Stage 3, we applied multiple extensiv visual plugins such as SAM [26], Grounding DINO and UniPose to demonstrate that our REF-VLM is extensible to more common architectures.

Config	Stage1	Stage2	Stage3-Keypoint	Stage3-gDINO	Stage3-SAM	Stage3-UniPose
visual encoder	frozen	frozen	frozen	frozen	frozen	frozen
vpt encoder	-	unfreeze	unfreeze	unfreeze	unfreeze	unfreeze
projector	unfreeze	unfreeze	unfreeze	unfreeze	unfreeze	unfreeze
LLM	frozen	unfreeze	unfreeze	unfreeze	unfreeze	unfreeze
box decoder (meta)	-	unfreeze	-	-	-	-
mask decoder (meta)	-	unfreeze	-	-	-	-
keypoint decoder (meta)	-	-	unfreeze	-	-	-
box decoder (gDINO)	-	-	-	unfreeze	-	-
mask decoder (SAM)	-	-	-	-	unfreeze	-
keypoint decoder (UniPose)	-	-	-	-	-	unfreeze
learning rate	1e-5	2e-6	2e-5	2e-5	2e-5	2e-5
optimizer	AdamW	AdamW	AdamW	AdamW	AdamW	AdamW
warmup ratio	0.03	0.03	0.03	0.03	0.03	0.03
weight decay	0	0	0	0	0	0
max norm	1	1	1	1	1	1
input resolution	336^2	336^2+512^2	336^2+512^2			
batch size per GPU	16	16	16	16	16	16
numerical precision	bfloat16	bfloat16	bfloat16	bfloat16	bfloat16	bfloat16
GPUs for training	$64 \times A800$ (80G)	$64 \times A800$ (80G)	$8 \times A800$ (80G)	$8 \times A800$ (80G)	$8 \times A800$ (80G)	$8 \times A800$ (80G)

Table 15. **Summary of datasets used in the whole training process.** Stage-1 datasets focus on visual understanding tasks, while in Stage-2 and Stage-3 we not only train the visual understanding tasks such as image captioning, VQA, but also target specific downstream density prediction tasks.

Training Stage	Datasets
Stage1	Visual Genome [27], Visual7W [78], llava-Instruct [33], VQAv2 [3], COCO [30], Flickr30k-Entities [42], RefCOCO [25], RefCOCO+ [25], RefCOCOg [25], VCR [69]
Stage2	COCO [30], VQAv2 [3], Grand [45], GRIT [41], RefCOCO [25], RefCOCO+ [25], RefCOCOg [25], COCO-Interactive [73], Osprey [68], Visual Genome [27], Visual7W [78], Flickr30k-Entities [42], LLaVA-Grounding [71], PNG [22], OpenPSG [77]
Stage3-Keypoint	COCO-Keypoint [30]
Stage3-gDINO	Grand [45], GRIT [41], RefCOCO [25], RefCOCO+ [25], RefCOCOg [25]
Stage3-SAM	Grand [45], RefCOCO [25], RefCOCO+ [25], RefCOCOg [25], COCO-REM [49], ADE20k [76], CityScapes [15]
Stage3-UniPose	COCO-Keypoint [30]

plugins separately. This demonstrated that our model could not only accommodate custom-designed decoders trained from scratch but also effectively leverage state-of-the-art

(SOTA) visual decoders. For each separate training process for different visual decoders, We set the learning rate to $2e - 5$ and trained the decoder for 5 epochs, using a batch

Table 16. **Total Data Volume and Data Ratios Across Different Training Stages.** We present the data ratios used in the three distinct training stages. In each stage, the model undergoes joint training on these datasets to develop multi-task capabilities.

Task	Stage1	Stage2	Stage3-Keypoint	Stage3-gDINO	Stage3-SAM	Stage3-UniPose
Visual Understanding	55.85%	26.22%	-	-	-	-
Referring Expression	25.58%	40.57%	-	33.41%	32.91%	-
Grounded Conversation Generation (GCG)	20.29%	14.01%	-	26.51%	23.03%	-
Interactive Grounding	-	2.90%	-	-	-	-
Open-Vocabulary Identification	-	16.30%	-	40.08%	44.06%	-
Keypoint Detection	-	-	100%	-	-	100%
Total Number	4,241,680	8,091,372	109,289	1,545,982	2,165,892	109,289

size of 16 per GPU.

E. Freeform Open-Vocabulary Identification

Compared to existing MLLMs [56, 58, 73], our REF-VLM offers greater flexibility and freedom in Open-Vocabulary Identification tasks. We therefore propose a new, more flexible task format called **Freeform Open-Vocabulary Identification** and introduce a corresponding evaluation metric, **mAP Similarity (mAP_S)**, specifically designed for this task.

E.1. Task Definition

In many open-vocabulary identification tasks that current MLLMs can perform [56, 58, 73], users are typically required to input relevant category information about the image in the prompt. This category information serves as input features for the prompt encoder, allowing the downstream visual decoder to execute detection and segmentation tasks based on the prompt. However, the VT-Instruct dataset adheres to the flexibility of the REF-VLM model when constructing such tasks. Users only need to provide a simple prompt like “Please segment/detect the objects in the image <image>.” to perform downstream detection and segmentation tasks. This approach eliminates the need for specific category information in the prompt, offering greater freedom and flexibility for these tasks. Therefore, we propose a new type of Open-Vocabulary Identification task called the **Freeform Open-Vocabulary Identification task**. In this task, open-set detection is carried out with enhanced flexibility, allowing users to omit specific category details in the prompt.

E.2. mAP Similarity (mAP_S)

Instead of the calculating mAP as our evaluation metric for Open-Vocabulary Identification tasks, we propose a new metric called mAP Similarity (mAP_S) to evaluate our REF-VLM performance. For traditional open-vocabulary models, they typically predict classes with a logit score by their classification head. However, instead of applying a classification head for each task, our REF-VLM leverages a large language model (LLM) to predict classes without generating any class logits. We therefore compute the similarity score

between REF-VLM’s class predictions and all ground truth class names. We then assign the class label based on the highest similarity, using this similarity score in place of the traditional confidence score.

For the implementation of mAP_S, we define the phrases predicted by the LLM as $p_i \in p_1, p_2, p_3, \dots, p_k$, where k denotes the number of LLM predictions. The ground truth classes are denoted as $c_i \in c_1, c_2, c_3, \dots, c_n$, where n is the total number of ground truth classes for the dataset. We first use the CLIP-Large-14-336 model to compute the text embeddings e , as shown in Equation (10). Next, we compute the cosine similarity score between each p_i and c_i as in Equation (11). The class of our predicted phrase is assigned based on the maximum similarity score and its corresponding index, which also serves as the logit score for the prediction.

$$e_{p_i} = \text{CLIP}(p_i), e_{c_i} = \text{CLIP}(c_i). \quad (10)$$

$$s_{max}, id_{max} = \max(\text{Cosine_Similarity}(e_{p_i}, e_{c_i})). \quad (11)$$

F. More Results

F.1. More Experimental Results

Referring Expression Segmentation (RES) For the Referring Expression Segmentation (RES) task, we evaluate REF-VLM on the RefCOCO, RefCOCO+, and RefCOCOg test and validation datasets by calculating the cumulative IOU (cIOU) as proposed by [32]. REF-VLM with meta plugins, trained from scratch, achieves results in both zero-shot and fine-tuned settings that are comparable to recent methods like LISA [28], which utilized pretrained backbones such as SAM (see Table 20). The results show that the performance of our REF-VLM trained from scratch is slightly lower than that of PixelLM [46], primarily due to PixelLM’s use of the CLIP-ViT-H visual encoder, which has significantly more parameters than ours (see Table 13). Additionally, to demonstrate that REF-VLM is not only capable of using custom-designed components but also can extend to current VGMs, we employed SAM as an external plugin for our mask decoder. By loading the pretrained weights from SAM and

Table 17. **Prompt template for evaluating different kind of tasks.** For different evaluation tasks, we utilized distinct prompt templates. During the actual training process, to ensure the model’s generalization across tasks, we constructed at least 100 templates for each subtask.

Task	Template
Caption	<image>Please describe the image in detail.
VQA	Please take a look at the image <image>and promptly provide an answer for <question>.
GCG-Mask	Describe the setting of the image <image>and offer masks for each visible object.
GCG-Box	Please describe the image <image>and detect relevant bounding boxes.
REC	What are the coordinates of <referring expression>in the image<image>?
RES	Provide a segmentation mask for <referring expression>in the picture <image>.
REG	For the given image <image>, can you provide a unique description of the area <mask>?
IG-Mask	Please generate a mask based on the region <region>in the image <image>.
FOVD	Please detect bounding boxes in the image<image>.
FOVS	Please segment objects in the image<image>.
Keypoint Detection	Please detect all the people and visualize all the keypoints in the image<image>.

Table 18. **Comparison of interactive grounding performance on segmentation task.** The task is evaluated on the COCO-Interactive [73] validation dataset. The evaluation metrics for interactive grounding are mIoU and cIoU.

Model	Decoder	Scratch	Type	Point		Scribble		Box		Mask	
				mIoU	cIoU	mIoU	cIoU	mIoU	cIoU	mIoU	cIoU
SAM-B [26]	-	✓	VGM	48.7	33.6	-	-	73.7	68.7	-	-
SAM-L [26]	-	✓		51.8	37.7	-	-	76.6	71.6	-	-
SEEM-B [80]	-	✓		47.8	57.8	43.0	44.0	44.9	42.1	48.4	65.0
PSALM [73]	Mask2Former	✗	MLLM	64.3	74.0	66.9	80.0	67.3	80.9	67.6	82.4
VisionLLMv2 [56]	GroundingDINO	✗		65.4	70.9	66.8	77.2	74.2	83.2	67.9	83.8
REF-VLM (meta)	Mask Decoder	✓		62.8	70.4	59.8	60.2	71.2	73.7	66.3	77.5
REF-VLM (external)	SAM	✗		65.6	75.2	68.3	79.4	74.9	84.6	68.2	83.7

Table 19. **Comparison of Referring Expression Comprehension (REC) performance.** REC is evaluated by IOU@0.5 Accuracy. VGM represents vision generalist model and MLLM represents multimodal large language model.

Model	Type	RefCOCO			RefCOCO+			RefCOCOg	
		Test-A	Test-B	Val	Test-A	Test-B	Val	Test	Val
OFA-L [51]	VGM	83.7	76.4	76.4	76.0	61.8	68.3	67.6	80.0
MAttNet [67]		80.4	69.3	80.0	70.3	56.0	64.9	67.0	76.4
UNITER [10]		87.0	74.2	81.4	81.5	66.7	75.9	68.7	74.0
VILLA [20]		87.5	74.8	82.4	81.5	66.8	76.2	76.7	76.2
MDETR [24]		89.6	81.4	86.8	84.1	70.6	79.5	80.9	81.6
GroundingDINO-T [36]		91.9	86.0	89.2	87.4	74.7	81.1	84.9	85.2
GroundingDINO-L [36]		93.2	88.2	90.6	89.0	75.9	82.8	87.0	86.1
Kosmos-2 [41]		57.4	47.3	52.3	50.7	42.2	45.5	61.7	60.6
Shikra [9]	MLLM	90.6	80.2	87.0	87.4	72.1	81.6	82.2	82.3
Ferret [66]		91.4	82.5	87.5	87.4	73.1	80.8	84.8	83.9
NeXT-Chat [70]		90.0	77.9	85.5	84.5	68.0	77.2	79.8	80.1
MiniGPTv2-7B [8]		91.3	84.3	88.1	85.5	73.3	79.6	84.3	84.2
Qwen-VL-7B [5]		92.3	84.5	88.6	88.6	76.8	82.8	86.3	86.0
VistaLLM [43]		91.5	83.0	88.1	89.8	74.8	82.9	84.4	83.6
VisionLLMv2 [56]		93.1	87.1	90.0	87.3	74.5	81.1	84.8	83.9
LION-12B [7]		93.0	85.6	89.8	89.2	78.1	84.0	85.7	85.5
REF-VLM		93.7	89.1	90.8	88.3	77.6	81.7	87.1	87.0

Table 20. **Comparison of Referring Expression Segmentation (RES) performance.** The ‘‘Decoder’’ column refers to the visual decoder utilized by the MLLM for performing RES tasks. * indicates that the visual decoder is custom-designed and trained from scratch. The performance of RES is evaluated using cumulative IoU (cIoU) as proposed by [32].

Model	Decoder	Scratch	Type	RefCOCO			RefCOCO+			RefCOCOg	
				Test-A	Test-B	Val	Test-A	Test-B	Val	Test	Val
MCN [37]	-	✓	VGM	64.2	59.7	62.4	55.0	44.7	50.6	49.4	49.2
VLТ [17]	-	✓		70.5	65.2	67.5	61.0	50.1	56.3	57.7	55.0
RELA [32]	-	✓		76.5	70.2	73.8	71.0	57.7	66.0	66.0	65.0
X-Decoder [79]	-	✓		-	-	-	-	-	-	-	64.6
SEEM-L [80]	-	✓		-	-	-	-	-	-	-	65.7
UNINEXT-H [63]	-	✓		83.4	81.3	82.2	76.4	66.2	72.5	76.4	74.7
GLEE-Pro [55]	-	✓		-	-	80.0	-	-	69.6	-	72.9
LISA-7B [28]	SAM	✗	MLLM	72.3	79.1	74.9	70.8	58.1	65.1	70.6	67.9
PixelLM [46]	Mask Decoder*	✓		76.5	68.2	73.0	71.7	58.3	66.3	70.5	69.3
PixelLLM [61]	SAM	✗		78.5	74.4	76.9	72.1	64.5	69.2	72.4	70.7
AnyRef	SAM	✗		79.9	74.2	76.9	73.5	61.8	70.3	70.7	70.0
NExT-Chat [70]	SAM	✗		78.9	69.5	74.7	71.9	56.7	65.1	67.0	67.0
VITRON [19]	SEEM	✗		78.7	71.6	74.4	72.1	57.8	66.3	67.3	67.2
GroundHOG [72]	Mask2Former	✗		79.9	75.7	78.5	75.0	64.9	70.5	74.6	74.1
GLaMM [45]	SAM	✗		83.2	76.9	79.5	78.7	64.6	72.6	74.9	74.2
VisionLLMv2 [56]	GroundingDINO	✗		82.3	77.0	79.2	75.8	61.8	68.9	74.8	73.3
REF-VLM (meta)	Mask Decoder*	✓		73.4	63.9	69.0	70.8	56.2	62.3	65.8	65.0
REF-VLM (external)	SAM	✗	82.9	76.8	81.2	77.6	63.4	73.1	75.0	74.6	

fine-tuning it on our VT-Instruct datasets, we found that REF-VLM with the external plugin outperforms current MLLMs such as VisionLLMv2 [56], GLaMM [45], and demonstrates comparable performance to the Generalist Model such as UNINEXT-H [63].

For the Referring Expression Comprehension (REC) task, we compare our REF-VLM with current MLLMs capable of generating referring boxes based on specific prompts in both zero-shot and fine-tuned settings. The metric used for REC evaluation is IoU@0.5. As shown in Table 19, REF-VLM demonstrates superior performance in the REC task compared to other MLLMs.

Interactive Grounding For this task, we evaluate using the prompt, ‘‘Please generate a mask based on the region <region> in the image <image>.’’ where <region> is replaced with visual prompts such as points, scribbles, boxes, or masks. The results presented in Table 18 show that our REF-VLM with meta plugins outperforms both SAM [26] and SEEM-B [80] across point, scribble, box, and mask settings, achieving performance comparable to PSALM, which utilizes pretrained Swin-T and Mask2Former weights in these configurations. Furthermore, our REF-VLM with external plugins achieves superior performance compared to VisionLLMv2 [56] and PSALM [73].

Table 21. Comparison of different configurations of VPT encoders on RefCOCOg validation dataset.

Method	CIDEr	Meteor	Params
Osprey [68]	78.5	12.0	6.55M
Use Mask Token	77.9	12.0	1024
No Mask Token	78.8	12.1	0

Table 22. Comparison of different configurations of Matching Strategy on COCOREM Test dataset.

Method	AP50	AP75	AP[50:95]	AR[50:95]
No-Matcher	12.4	1.4	4.0	16.4
Use Matcher	12.7	2.6	4.5	19.3

F.2. More Ablation Results

Different Configuration of VPT Encoding Strategy. Our parameter-free VPT encoder configuration outperforms alternatives as shown in Table 21. Without mask tokens, our approach achieves the best CIDEr (78.8) and Meteor (12.1) scores with zero additional parameters, using block-wise dot products between masks and visual features with position encoding and shared projectors. Conversely, Osprey [68] uses unblocked dot products (N=1) and separate projections, requiring 6.55M parameters while yielding inferior results. Our efficient design delivers both superior

performance and exceptional cross-architecture adaptability.

Ablation of Group Hungarian Matcher

We conduct experiments with Group Hungarian Matching on the more challenging task of freeform object detection. Both experiments are trained for 5 epochs on the COCO-REM dataset, with comparative results shown in Table 1. The Group Matcher demonstrates superior performance across AP and AR metrics, particularly showing significant improvement in AP75, indicating its effectiveness in enhancing box regression accuracy.

G. More Visualization Results

Prompt

Provide a simple description of this photograph. I would like to hear a more thorough description.

VD-CoT

```
<Task>
Unit decode (False).
</Task>
```



Answer with Triplets

A group of people, including children, are gathered on a brick wall, some holding umbrellas and backpacks while others wear dresses, sunhats, and shirts. A man wearing a hat and a pink-shirted person are also visible. In the background, a large brick building can be seen, and the scene outside provides a view.

Table 23. **An Example of VD-CoT Applied to the Visual Caption Task.** In this task, only textual responses are required, and no operations on image information are needed. Therefore, in the generation of VD-CoT, Unit decode is set to False, and no visual-related special tokens are generated. Similarly, in the result of Answer with Triplets, there are no decoded triplets related to visual content.

Prompt

Please identify each object in the image.

VD-CoT

```
<Task>
Unit decode (True). Class name, target unit and number:
- Name: car Unit: box Num: 10
- Name: skyscraper Unit: box Num: 1
- Name: barricade Unit: box Num: 1
- Name: city Unit: box Num: 1
- Name: street Unit: box Num: 1
</Task>
```



Answer with Triplets

```
<Phrase>car</Phrase> (<Unit>box</Unit>[0]<REF>[1]<REF>[2]<REF>[3]<REF> [4]<REF>
[5]<REF>[6]<REF>[7]<REF>[8]<REF>[9]<REF>),
<Phrase>skyscraper</Phrase> (<Unit>box</Unit>[0]<REF>),
<Phrase>barricade</Phrase> (<Unit>box</Unit>[0]<REF>),
<Phrase>city</Phrase> (<Unit>box</Unit>[0]<REF>),
<Phrase>street</Phrase> (<Unit>box</Unit>[0]<REF>).
```

Table 24. **An Example of VD-CoT Applied to the Object Detection Task.** VD-CoT analyzes the visual content and generates decoding triplets to identify objects in the image. The special tokens and references have been included for clarity.

Prompt

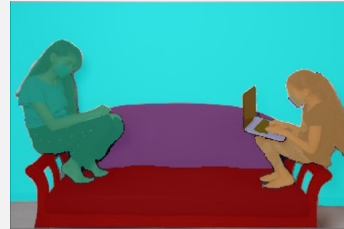
Delineate areas of the image into semantic segments.

VD-CoT

<Task>

Unit decode (True). Class name, target unit and number:

- Name: couch Unit: mask Num: 1
- Name: computer keyboard Unit: mask Num: 1
- Name: mask Unit: mask Num: 2
- Name: person Unit: mask Num: 2
- Name: sofa Unit: mask Num: 1
- Name: monitor (computer equipment) computer monitor Unit: mask Num: 1



</Task>

Answer with Triplets

<Phrase>couch</Phrase> (<Unit>mask</Unit>[0]<REF>),
<Phrase>computer keyboard</Phrase> (<Unit>mask</Unit>[0]<REF>),
<Phrase>mask</Phrase> (<Unit>mask</Unit>[0]<REF>[1]<REF>),
<Phrase>person</Phrase> (<Unit>mask</Unit>[0]<REF>[1]<REF>),
<Phrase>sofa</Phrase> (<Unit>mask</Unit>[0]<REF>),
<Phrase>monitor (computer equipment) computer monitor</Phrase>
(<Unit>mask</Unit>[0]<REF>).

Table 25. An Example of VD-CoT Applied to the Open-Vocabulary Segmentation Task. VD-CoT analyzes the visual content and generates decoding triplets for semantic segmentation of the image. Special tokens and references are provided for clarity.

Prompt

Please pinpoint the egg yolk in the image and provide the dimensions of its bounding box.

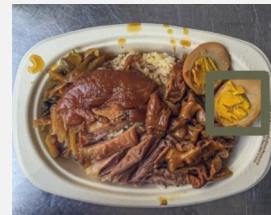
VD-CoT

<Task>

Unit decode (True). Class name, target unit and number:

- Name: target Unit: box Num: 1

</Task>



Answer with Triplets

<Phrase>target</Phrase> (<Unit>box</Unit>[0]<REF>).

Table 26. An Example of VD-CoT Applied to the Referring Expression Comprehension Task. VD-CoT analyzes the visual content and generates decoding triplets to identify the target (egg yolk) and its bounding box dimensions in the image.

Prompt

How do you create a segmentation mask for a white boat in the water in the image?

VD-CoT

<Task>
Unit decode (True). Class name, target unit and number:
- **Name:** target **Unit:** mask **Num:** 1
</Task>



Answer with Triplets

<Phrase>target</Phrase> (<Unit>mask</Unit>[0]<REF>).

Table 27. An Example of VD-CoT Applied to the Referring Expression Segmentation Task. VD-CoT analyzes the visual content and generates decoding triplets to identify the target (white boat) and creates its segmentation mask in the image.

Prompt

What defining features can you describe for the area [VPT] in the image?

VD-CoT

<Task>
Unit decode (False).
</Task>



Answer with Triplets

The cabinet is closed.

Table 28. An Example of VD-CoT Applied to the Referring Expression Generation Task. VD-CoT analyzes the visual content and generates descriptive features for the given area [VPT] in the image.

Prompt

Segment the region based on the region [VPT] in the image, and illustrate the resulting mask.

VD-CoT

<Task>
Unit decode (True). Class name, target unit and number:
- **Name:** boat **Unit:** mask **Num:** 1
</Task>



Answer with Triplets

<Phrase>boat</Phrase> (<Unit>mask</Unit>[0]<REF>).

Table 29. An Example of VD-CoT Applied to the Interactive Grounding Task. VD-CoT analyzes the visual content, segments the region [VPT], and generates a mask for the identified object (boat) in the image.

VQA



Please describe the image in more details.



Describe the main features of the image.

A man sitting on a concrete block on the beach.



REF-VLM



Where is the man ?

The man is sitting on a concrete block or cement slab at the beach.



REF-VLM

In the image, a man is sitting on a concrete block near the beach, enjoying the view of the ocean. He is wearing shorts and a white shirt, and he appears to be relaxing and taking in the scenery.

There are several other people in the scene, some of whom are standing near the beach, while others are further away. A skateboard is visible on the ground, suggesting that the man might have been skateboarding before taking a break on the concrete block.

In the background, a boat can be seen floating on the water, adding to the beach atmosphere.



REF-VLM



Please give me more details about image.



Tell me the main thing in the image.

A man and a dog playing with a frisbee in front of a crowd.



REF-VLM



Where is the dog ?

The dog is in the air, jumping to catch a frisbee.



REF-VLM

In the image, a large crowd of people is gathered in a grassy field, watching a dog perform an impressive trick. The dog is jumping high in the air, attempting to catch a frisbee. The crowd is captivated by the dog's skill and athleticism.

There are numerous people in the scene, with some standing closer to the dog and others further away. Some of the spectators are holding frisbees, likely waiting for their turn to throw them for the dog to catch. The atmosphere is lively and filled with excitement as the dog showcases its talent.



REF-VLM

Figure 9. The Visual Understanding Results of REF-VLM.



Figure 10. **The Detection Results of REF-VLM.** The text color in the model’s responses corresponds to the bounding box colors of the detected objects in the images. For example, in the top-right image, the model detects two categories: “person” and “dress.” The “person” category contains two instances, represented by [0]<REF> and [1]<REF>, while the “dress” category contains one instance, represented by [0]<REF>.



Figure 11. **The Segmentation Results of REF-VLM.** The figure illustrates the segmentation and GCG segmentation outputs generated by REF-VLM. The text corresponds to the mask colors of the segmented objects in the images. For example, in the top-left image, the model segments three categories: “stool,” “person,” and “grassy field.” The “person” category contains two instances, represented by [0]<REF> and [1]<REF>, while the “stool” category contains one instance, represented by [0]<REF>. The background, labeled as “grassy field,” is also represented by [0]<REF>.

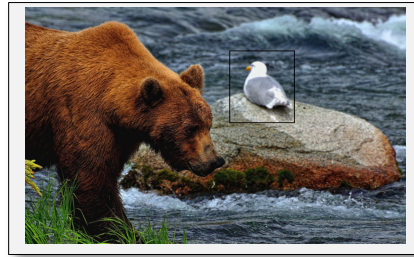
Grounding Detection



Text as the Prompt



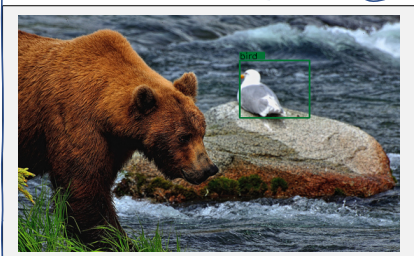
Please identify the position of bear in the image and give the bounding box coordinates.



Box as the Prompt



Please tell me what animal is in the box **<area>**?



Text as the Prompt



Please locate the man in the image and give the bounding box.



Box as the Prompt



Please tell me what category is in the box **<area>** and fix the box.



Figure 12. **The Grounding Detection Results of REF-VLM.** We use the textual prompts and visual box prompts for grounding detection tasks. In the first row (left), a textual prompt instructs the model to locate the object “bear” mentioned in the sentence. The second row displays the result, where the model successfully detects the location of the bear using a **bounding box**. In the first row (right), a bounding box around a bird is provided as a visual prompt. The textual query uses the special token **<area>** to refer the boxed region in the image. The second row (right) shows the model’s output, correctly identifying the object in the boxed region as a “bird.”



Figure 13. **The Grounding Segmentation Results of REF-VLM.** We use the textual prompts and visual box prompts for grounding segmentation tasks. In the first row (left), a textual prompt instructs the model to segment the **middle bird** in the center of the image. The second row (left) shows the segmentation result for the **middle bird** produced by the model based on the textual prompt. In the first row (right), bounding boxes around two birds are provided as visual prompts, and the textual prompt includes a special symbol **<area>** to indicate the region for segmentation. The second row (right) displays the segmentation results for the **left bird** and **right bird** based on two types of prompts.